



**Technische Universität München**

**TUM School for Medicine and Health**

***Investigating early fate decisions of exhausted CD8<sup>+</sup> T cells by in vivo single cell fate mapping***

Theresa Sophie Busch

Vollständiger Abdruck der von der TUM School of Medicine and Health der Technischen Universität München zur Erlangung einer

**Doktorin der Medizin (Dr. med.)**

genehmigten Dissertation.

Vorsitz: Prof. Dr. Lars Mägdefessel

Prüfer der Dissertation:

1. Priv.-Doz. Dr. Veit Buchholz

2. Prof. Dr. Thomas Korn

Die Dissertation wurde am 12.07.2023 bei der Technischen Universität München eingereicht und durch die TUM School of Medicine and Health am 03.01.2024 angenommen.

## Parts of this thesis have previously been published:

### ***Early diversification during chronic infection generates exhaustion-receptive and -resistant T cell subsets***

Lorenz Kretschmer<sup>1\*</sup>, Albulena Toska<sup>1\*</sup>, Theresa Busch<sup>1\*</sup>, Immanuel Andrä<sup>1</sup>, Dietmar Zehn<sup>2</sup>,  
Michael Flossdorf<sup>1</sup>, Veit R. Buchholz<sup>1</sup>

#### Affiliations:

1

Institute for Medical Microbiology, Immunology and Hygiene, Technical University of Munich (TUM), Munich, Germany

2

Division of Animal Physiology and Immunology, School of Life Sciences Weihenstephan, Technical University of Munich (TUM), Freising, Germany \*these authors contributed equally

Presented at the International Conference for Lymphocyte Engineering, 31.03.-02.04.2022, Munich

# Table of contents

<b>1. Introduction</b>	<b>1</b>
1.1. Organization of the mammalian immune system	1
1.2. Dynamics of antiviral T cell responses	2
1.3. CD8 <sup>+</sup> T-cell exhaustion in settings of persistent antigenic stimulus	3
1.4. Developmental framework of functional and exhausted CD8 <sup>+</sup> T cells	6
1.5. Kinetics of different LCMV-infections	8
1.6. Single cell <i>in vivo</i> fate mapping as a tool to determine lineage relationships	9
<b>2. Aim of this thesis</b>	<b>13</b>
<b>3. Materials and Methods</b>	<b>14</b>
3.1. Materials	14
3.1.1. Reagents	14
3.1.2. Buffers and Media	15
3.1.3. Antibodies	16
3.1.4. Equipment	17
3.1.5. Software	18
3.2. Methods	18
3.2.1. Mice	18
3.2.2. Preparation of cell suspensions from various organs	18
3.2.3. Staining protocols for FACS analysis of cell surface antigens	19
3.2.4. Staining protocols for FACS analysis of intracellular antigens	20
3.2.5. Restimulation and measurement of cytokine production	20
3.2.6. Flow cytometric cell sorting	21
3.2.7. FACS-based analysis	22
3.2.8. Viruses and infections	22
3.2.9. Cell lines	22
3.2.10. Virus propagation and quantification.	22

3.2.11. Data visualization and statistics	23
3.2.12. Biomathematical calculation and modelling	24
<b>4. Results</b>	<b>25</b>
<b>4.1. Single-cell <i>in vivo</i> fate mapping in acute and chronic infection</b>	<b>25</b>
4.1.1. Establishing LCMV as a murine model system to study immune responses against acute and chronic infections	25
4.1.2. Identifying distinct subsets of exhausted CD8 <sup>+</sup> T cells	27
4.1.3. Single cell <i>in vivo</i> fate mapping in acute and chronic infection	30
<b>4.2. scRNA-seq and RNA velocity analyses during the early phase of acute and chronic LCMV infection</b>	<b>33</b>
<b>4.3. Adoptive re-transfer of emerging CD8<sup>+</sup> T cell subsets to test developmental relationships proposed by scRNA-seq</b>	<b>35</b>
4.3.1 Early adoptive retransfer experiments to explore the developmental capacity of CD8 <sup>+</sup> T cells exposed to chronic infection	35
4.3.2 Transfer of acutely primed, terminally differentiated effector cells into chronic infection	37
<b>4.4. Longitudinal tracking of single cell progeny into the late phase of chronic infection</b>	<b>39</b>
<b>5. Discussion</b>	<b>42</b>
5.1. Progressive differentiation of exhausted CD8 <sup>+</sup> T cells	42
5.2. Clonal burst size is restricted in LCMV-CI13	43
5.3. Terminal effector differentiation is impaired in chronic infection	44
5.4. KLRG-1 <sup>+</sup> effector cells might hold immunopathogenic potential in the setting of chronic infection	45
5.5. CD8 <sup>+</sup> T cells regain functionality after clearance of LCMV-CI13 from the blood	46
<b>6. Summary</b>	<b>48</b>
<b>7. Bibliography</b>	<b>50</b>
<b>8. Acknowledgements</b>	<b>65</b>

## Index of figures

<b>Figure 1:</b>	Schematic depiction of the dynamics of antigen load and specific T cell response in acute and chronic infection.	3
<b>Figure 2:</b>	The „hallmarks“ of exhausted CD8 <sup>+</sup> T cells.	5
<b>Figure 3:</b>	Developmental framework of early functional and exhausted CD8 <sup>+</sup> T cell responses.	7
<b>Figure 4:</b>	Relation between single cell- and population-derived CD8 <sup>+</sup> T cell responses.	10
<b>Figure 5:</b>	Models of CD8 <sup>+</sup> T cell diversification.	11
<b>Figure 6:</b>	P14 T cells mount phenotypically distinct responses after acute and chronic LCMV infection.	25
<b>Figure 7:</b>	The first week of LCMV infection sees the development of phenotypically diverse CTL subsets.	27
<b>Figure 8:</b>	Expression of CX3CR1 and TCF1 delineates three functionally distinct subsets of CD8 <sup>+</sup> T cells.	29
<b>Figure 9:</b>	Single cell <i>in vivo</i> fate mapping in acute and chronic LCMV infection.	30
<b>Figure 10:</b>	Tracking of individual fates reveals impaired differentiation of terminal effectors and restricted variability in clonal burst size in chronic LCMV infection.	32
<b>Figure 11:</b>	sc-RNA-seq velocity analysis reveals distinct differentiation trajectories within the TCF7 <sup>-</sup> cell compartment in acute and chronic LCMV infection.	34
<b>Figure 12:</b>	MPs and EEs show considerable developmental plasticity at day four and half of CI13 infection.	36
<b>Figure 13:</b>	Mature, acutely primed TEs appear exhaustion-resistant.	38
<b>Figure 14:</b>	Single cell fate mapping reveals that individual T cell families can revert to a functional state towards the late stages of LCMV CI13 infection.	39

## Abbreviations

ACT	Ammonium chloride-Tris
APC	Antigen presenting cell
APC	Allophycocyanin
BSA	Bovine serum albumin
CD	Cluster off differentiation
CM	Central memory
CMP	Central memory precursor
CTL	Cytotoxic T lymphocyte
CV	Coefficient of variation
DC	Dendritic cell
DMSO	Dimethyl sulfoxide
DNA	Desoxyribonucleic acid
EDTA	Ethylendiamintetraacetate
EMA	Ethidium monoazide bromide
EM	Effector memory
EMP	Effector memory precursor
eps	events per second
FACS	Fluorescence activated cell sorting
FCS	Fetal calf serum
FITC	Fluorescein- isothiocyanate
GFP	Green fluorescent protein
h	hours

IL	Interleukin
IL-2	Interleukin 2
IFN- $\gamma$	Interferon $\gamma$
irAE	immune related adverse event
i.p.	Intraperitoneal
i.v.	Intravenous
KO	Knockout
LCMV	Lymphocytic choriomeningitis virus
LCMV -Arm	Lymphocytic choriomeningitis virus Armstrong strain
LCMV-Cl13	Lymphocytic choriomeningitis virus Clone 13 strain
MHC	Major histocompatibility complex
min	Minutes
MP	Memory precursor
MPEC	Memory precursor effector cell
PAMP	Pathogen associated molecular pattern
PBS	Phosphate buffered saline
PE	Phycoerythrin
PECy7	Phycoerythrin-Cyanine 7
PFA	Paraformaldehyde
PFU	Plaque forming units
PI	Propidium iodide
p.i.	Post infection
p:MHC-I/II	Peptide:MHC-I/II
RBC	Red blood cell
rpm	Rounds per minute
RT	Room temperature

SC+	Medium supplement
SPF	Specific pathogen free
SLEC	Short lived effector cell
TCR	T cell receptor
TE	Terminal effector
T <sub>ex</sub>	Exhausted CD8 <sup>+</sup> T cell
TNF- $\alpha$	Tumor necrosis factor $\alpha$
Wt	Wild type

## 1. Introduction

### 1.1. Organization of the mammalian immune system

The mammalian immune system's response to a foreign, potentially pathogenic agent is executed by two distinct branches. The innate immune system can react without the prerequisite of an antecedent encounter. Activation of its cellular division is based on the interaction of Pattern Recognition Receptors (PRRs), such as Toll Like Receptors (TLRs), which are widely expressed across immune and non-immune cell types, with Pathogen Associated Molecular Patterns (PAMPs) (Murphy & Weaver, 2017). These cover a multitude of molecules, from structural components common to many microbes such as cell wall constituents or nucleic acids to hyaluronan or mitochondrial DNA as indicators of tissue damage, ensuring a sensitive and efficient reaction. Depending on the type of cell engaged, downstream signaling leads to either direct elimination by various means or amplification of the response by recruitment of further players; through direct cell-cell interaction as in the case of Dendritic Cells (DCs) and other professional Antigen Presenting Cells (APCs) or by production of proinflammatory cytokines like IL-1 $\beta$ , IL-6, Type I Interferons or TNF- $\alpha$ , thus forging a link to adaptive immunity. Other cellular mediators include unspecific antimicrobial peptides constitutively secreted at barrier sites, for example lysozyme or lactoferrin. (Murphy & Weaver, 2017)

In contrast, adaptive immunity operates in an antigen-specific manner. Lymphocytes express a T or B cell receptor (TCR/BCR), that exclusively binds a single epitope, together with receptor-associated proteins on their surface. In order to ensure reliable pathogen recognition, this necessitates a receptor repertoire matching the potential antigens in diversity. The required breadth is achieved by the process of somatic recombination, the arbitrary rearrangement of different gene cassettes. Rounds of positive and negative selection serve to ascertain sufficient reactivity and self-tolerance. Both lymphocytic lineages originate from hematopoietic stem cells in the bone marrow, and while B cells are selected there before emigrating to the secondary lymphoid organs for maturation, T cells undergo this process in the thymus. Two distinct T cell populations emerge: CD4<sup>+</sup> helper T cells, restricted by MHC-II and indispensable for orchestration of the immune response, and MHC-I expressing CD8<sup>+</sup> cytotoxic T cells equipped to lyse infected target cells (Murphy &

Weaver, 2017). B cells are the sole producers of antibodies and thus carry the humoral arm of adaptive immunity. Antibodies are soluble homologues of the BCR, existing in five different classes (isotypes) and are subject to somatic hypermutation to increase their efficacy. TCR crosslinking after antigen-binding serves as the first signal of T-cell activation. Costimulation via CD28/B7 and inflammatory cytokines are the second and third signal, respectively, with the latter profoundly dictating the type of immune reaction depending on the nature of the causative agent (Murphy & Weaver, 2017). Although large polysaccharides are sufficient to activate B-cells, they need CD4<sup>+</sup> help via interaction with p:MHC-II to induce isotype switch and form memory. Robust proliferation, also referred to as clonal expansion, of the activated lymphocytes ensues, compensating for the low number of antigen-specific precursors. The majority of these cells is short lived and dies once antigen is cleared, but a select few survive to facilitate rapid action in case of reencounter and convey long-term immunity. (Murphy & Weaver, 2017)

### **1.2. Dynamics of antiviral CD8<sup>+</sup> T cell responses**

During acute viral infection, a pool of naïve CD8<sup>+</sup> precursors is activated and undergoes vigorous proliferation, giving rise to large numbers of short-lived effector cells that clear the virus using their strong cytolytic potential. The subsequent contraction phase sees most of these cells die, with 5-10% remaining, intended to mediated lasting protective immunity (Kaech et al., 2002). These memory cells can undergo slow homeostatic proliferation driven by IL-7 (Schluns et al., 2000) and IL-15 (Zhang et al., 1998), persist in the absence of antigen and rapidly expand and execute effector functions upon rechallenge. A short antigenic stimulus has been proven sufficient to prompt memory formation, as opposed to optimal expansion of the primary response, which requires availability of cognate peptide for several days (Blair et al., 2011; Prlic et al., 2006; van Stipdonk, 2001). Which fate a T cell adopts seems to critically depend on the sum of inflammatory stimuli it receives as the third signal of activation, which operates by modulating its transcriptional program (Joshi et al., 2007; Takemoto et al., 2006; Cui et al., 2009). Examples of such signal three cytokines are IL-12 and Type I Interferons, which lengthen the period of proliferation after CD8 T cell activation by sustaining surface expression of the high-affinity IL-2 receptor (Starbeck-Miller et al., 2014).

However, a number of diseases exist which cannot be rapidly resolved but instead become chronic, resulting in unremittingly high levels of antigen and thus TCR stimulation, with

eventual exhaustion of the cellular immune response as the consequence (Zajac et al., 1998; Wherry et al., 2003; Utzschneider, Alfei, et al., 2016). Examples of such conditions in humans include HIV, chronic hepatitis B and C and the spectrum of malignancies (Bertoletti & Gehring, 2006; Ye et al., 2015; Gruener et al., 2001; Pauken & Wherry, 2015; Zarour, 2016). Different immunoevasive strategies allow viruses to sidestep their host's defenses and establish persistence (Virgin et al., 2009). Targeting CD8<sup>+</sup> T cells, these include epitope escape mutations (Allen et al., 2000) limiting immunogenicity by downregulating MHC-I expression (Scheppeler et al., 1989; Kerkau et al., 1989), disrupting processing of cognate peptide by inhibiting the ubiquitin/proteasome pathway (Levitskaya et al., 1997), disrupting pro-apoptotic signals (Irmler et al., 1997), tropism to immunoprivileged niches (Mueller et al., 2007) or promotion of immunosuppressive cytokine secretion, such as IL-10 (Brooks, Trifilo, et al., 2006).

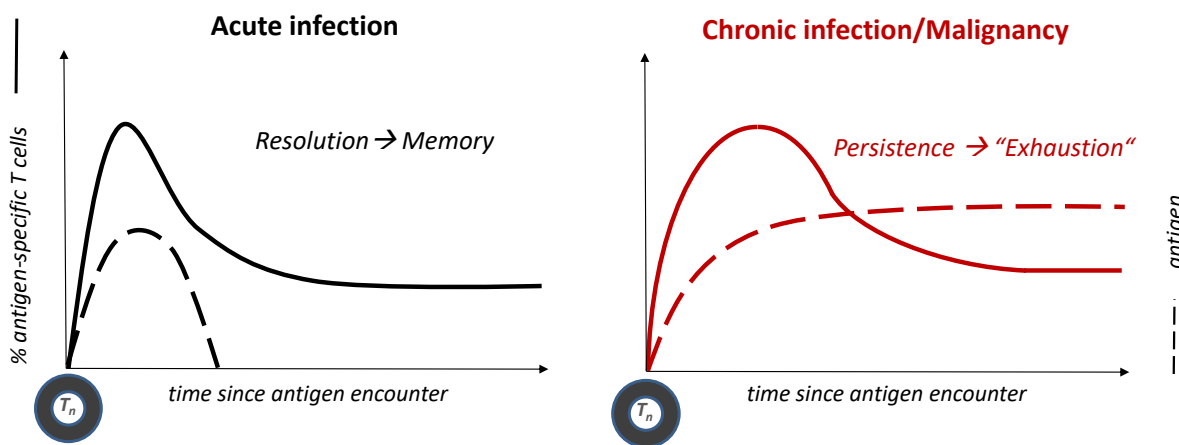


**Figure 1: Schematic depiction of the dynamics of antigen load and specific T cell response in acutely resolved and persistent conditions.** While viral antigen is cleared by the effector response in an acute infection, it persists at high levels in the chronic setting. (Modified from Wherry et al., 2004; McLane et al., 2019)

### 1.3. CD8<sup>+</sup> T cell exhaustion in settings of persistent antigenic stimulus

Prolonged antigenic stimulation eventually results in a considerable impairment of the antiviral T cell response. CD8<sup>+</sup> T cells are hyporesponsive and show reduced effector capacities. This state has been termed exhaustion and was first observed in mice infected with the Clone 13 strain of Lymphocytic Choriomeningitis Virus (LCMV) (Zajac et al., 1998). In this study, Zajac et al. found that in immunocompetent mice infected with Cl13, antigen-specific CD8<sup>+</sup> T cells persisted indefinitely, showed an activated phenotype (CD44<sup>high</sup>CD62L<sup>low</sup>) and proliferated but did not elaborate effector functions despite signs of

recent TCR-engagement (CD69<sup>+</sup>). These deficits were aggravated in the absence of CD4<sup>+</sup> help; both permanent deletion by genetic knockout as well as transient depletion by intravenous antibody application resulted in lifelong viremia and more severe dysfunction, as evaluated by IFN- $\gamma$  production. Contrastingly, the presence of a population of antigen-specific CD4<sup>+</sup> T cells early during infection allowed a fraction of CD8<sup>+</sup> T cells to remain functional and ultimately clear virus.

The deletion of cells specific for the dominant epitope during acute infection, NP396, ensued regardless of the host's CD4<sup>+</sup> status, and was later linked to its greater abundance and consequently more frequent TCR-engagement compared to GP33 (Wherry et al., 2003; van der Most et al., 1998). In fact, high antigen amount rather than TCR-affinity was identified to be the main driver of exhaustion in addition to type I interferons (Utzschneider, Alfei, et al., 2016; Zuniga & Harker, 2012; Richter et al., 2012; Mueller & Ahmed, 2009; Wu et al., 2016). Abrogation of cognate peptide at early stages can salvage the CTL response, as opposed to later time points when functional defects become irreversible (Richter et al., 2012; Shin et al., 2007; Blattman et al., 2009). Concurrently, in LCMV-Clone 13 infection in mice, we and others detected first effects of exhaustion on CD8<sup>+</sup> T cells by day 4-5- p.i. Only later, however, between one and two weeks p.i. do these appear to become permanent (Utzschneider et al., 2020). Considering the context of a chronic, potentially lifelong infection, the developmental program causing a hypofunctional immune system is initiated before any clinical signs of disease. Preventing excessive immunopathology during unchecked viral replication during the expansion phase of the T cell response has been suggested as a physiological purpose. (Aichele et al., 2022) With regard to malignancies, where features of exhaustion are also commonly observed (Iwai et al., 2002), this reading does not transfer directly, as in addition to the modifying properties of the tumor microenvironment, levels of antigens likely don't follow the same dynamics (Zarour, 2016; McLane et al., 2019; Schietinger et al., 2016).

Similar behavior was detected for human cytotoxic lymphocytes (CTL) in HIV (Day et al., 2006; Shankar et al., 2000), Hepatitis B (Bertoletti & Gehring, 2006; Ye et al., 2015) and C (Gruener et al., 2001) and various malignancies (Pauken & Wherry, 2015; Zarour, 2016). Owing to this significance for global health due to the possible impact on the progress and outcome of these conditions, CD8<sup>+</sup> T cell exhaustion has received considerable scientific

attention over the past two decades. Ensuing studies have defined the “hallmarks” of exhaustion (Figure 2). In addition to the sustained expression of potentially multiple coinhibitory receptors, foremost PD-1, but also LAG-3 or TIM-3, exhausted cells sequentially lose the ability to produce IL-2, TNF- $\alpha$  and lastly IFN- $\gamma$ , curtailing their effector functions and show metabolic impairment. A unique epigenetic landscape and transcriptome, controlled by the master-regulator TOX, mark them as a lineage distinct from classical effector and memory cells, prompting exhaustion to not to be understood as a mere dysfunction, but rather a differentional state adapted precisely to balance the needs for viral control and limiting cytotoxic activity and thus detrimental tissue damage in the continuous presence of high levels of antigen. Viral escape in chronic HIV infection and accelerated disease progression in the absence of antigen-specific CD8<sup>+</sup> T cells prove that these “hypofunctional” cells still contribute critically to viral control (Speiser et al., 2014).

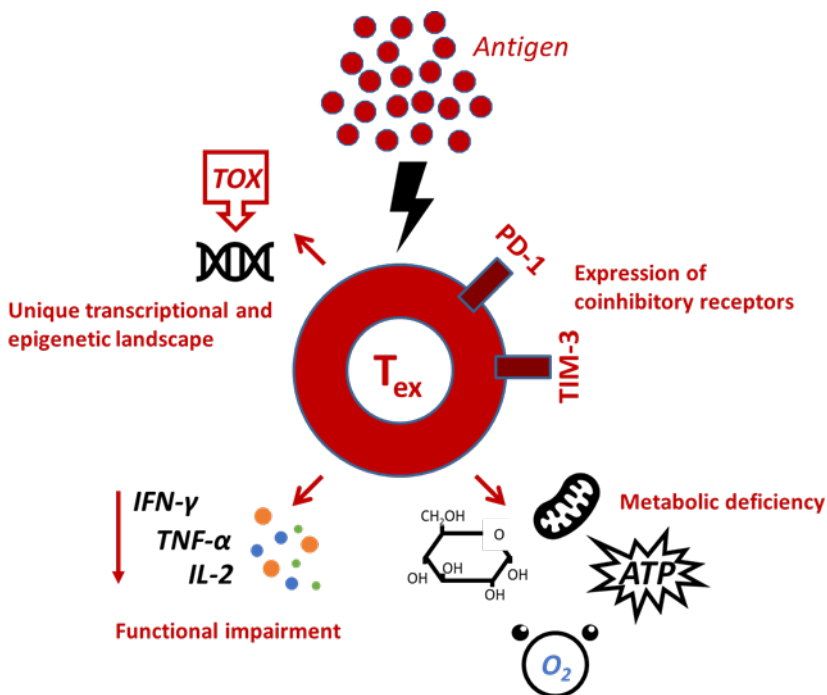


**Figure 2: The „hallmarks“ of exhausted CD8<sup>+</sup> T cells.** Chronic antigen exposure leads to expression of coinhibitory receptors, metabolic deficiency, functional impairment as well as a unique transcriptional and epigenetic landscape.

Next to resolving the question about the cause of exhaustion, the main therapeutic interest has been focused on developing strategies to realize its -at least partial- reversal and thus restoration of the immune response. In the context of chronic LCMV-infection, the coinhibitory receptor PD-1 as well as its therapeutic blockage, commonly referred to as checkpoint inhibition, have been investigated. Consistent with its role in restraining self-reactivity, this molecule has also been linked to autoimmunity (Okazaki et al., 2013).

Inhibiting interaction with its two known ligands - PD-L1, which is expressed across a diverse range of tissues and PD-L2, found only on professional APCs (Liang et al., 2003)- succeeded in expanding the population of antigen-specific CTLs and reinvigorating effector functions in LCMV Cl13 infection (Barber et al., 2006), and combination with IL-2 (West et al., 2013) or blocking of other inhibitory molecules such as LAG-3 amplified this effect, emphasizing that the pathways employed by these suppressive molecules are not redundant (Blackburn et al., 2009). The concept of “checkpoint inhibitor therapy” has established itself as a treatment regimen for several cancer entities. Although some patients benefit profoundly, more experience relapse within a few months of cessation, likely because T cells only undergo transient reactivation, whereas underlying epigenetic and transcriptional programs remain unaltered (Pauken et al., 2016; Ghoneim et al., 2017). At the same time, abrogating PD-1 signaling at the early stages of chronic LCMV infection leads to endothelial dysfunction and lethal circulatory failure in mice (Frebel et al., 2012), sharply accentuating the importance of its physiological role in averting immunopathology.

### **1.4. Developmental framework of functional and exhausted CD8<sup>+</sup> T cells**

Encounter with cognate peptide sets a naïve CD8<sup>+</sup> T cell on a pathway of linear differentiation. After activation, it initially converses into a TCMp (central memory precursor, CD27<sup>+</sup>CD62L<sup>+</sup>). TCMps generate TEMps (effector memory precursor, CD27<sup>+</sup>CD62L<sup>-</sup>), which in turn give rise to TEF (effector cells, CD27<sup>-</sup>CD62L<sup>-</sup>). Each transition is accompanied by an increase in proliferative activity and division speed (*Figure 3a*). TEF account for 90-95% of the antigen-specific population at the peak of the immune response (Buchholz et al., 2013). After contraction of the expanded T cell population, remaining TCMps and TEMps give rise to their respective memory lineages: quiescent and stemlike (Graef et al., 2014) TCM, which retain expression of both CD62L and CCR7, allowing them to home to lymphoid organs, and more cytotoxic TEM, scouting peripheral tissues (Sallusto et al., 1999). Such memory cells survive in the absence of antigen, undergo homeostatic proliferation driven by IL-7 and IL-15 (Schluns et al., 2000; Zhang et al., 1998), and have the ability to promptly expand and execute effector functions in response to secondary antigen encounter. Although the pool of exhausted CD8<sup>+</sup> T cells with its evenly high expression of PD-1, TOX and lack of effector population might seem homogeneous, varying biological properties have recently been identified. Several models for its division into functionally distinct T cell subsets have been

suggested. They agree on the common assumption of a synergism of at least two interconnected  $T_{ex}$  subsets, with less differentiated progenitors capable of self-renewal maintaining more terminally exhausted progeny (Figure 3b). Differences include the definition of additional transitory states between these two and the choice of key identifiers. T cell factor 1 (TCF-1), encoded by *TCF7*, is an effector of Wnt-signaling. It has important function in the development of thymocytes (Verbeek et al., 1995), is expressed on naïve T cells and downregulated after TCR-engagement in acute infection (Willinger et al., 2006). Ly108 can serve as an extracellular surrogate (Utzschneider, Charmoy, et al., 2016). *TCF-7*-deficient mice mount functional, if slightly quantitatively decreased, primary responses, but fail to form and maintain memory (Zhou et al., 2010; Jeannot et al., 2010). Its pivotal role in upholding  $CD8^+$  mediated immunity in chronic infection by sustaining the progenitor compartment has become widely accepted (Utzschneider, Charmoy, et al., 2016; Chen et al., 2019). Other indicators of this fate are the chemokine receptor CXCR5 or the transcription factors T-bet and, lately, BACH2. Tim-3, CD69, high levels of PD-1 and the transcription factor Eomes, on the other hand, have been shown to mark the more differentiated counterpart (Paley et al., 2012; He et al., 2016; Im et al., 2016; Beltra et al., 2020; Yao et al., 2021). Eomes and T-bet are reciprocally involved in not only regulating memory and effector differentiation in acute infection (Takemoto et al., 2006) but also execute similar influence over  $T_{ex}$  development (Paley et al., 2012; Doering et al., 2012). This has lately been traced back particularly to changes in their respective nuclear localization (McLane et al., 2021).

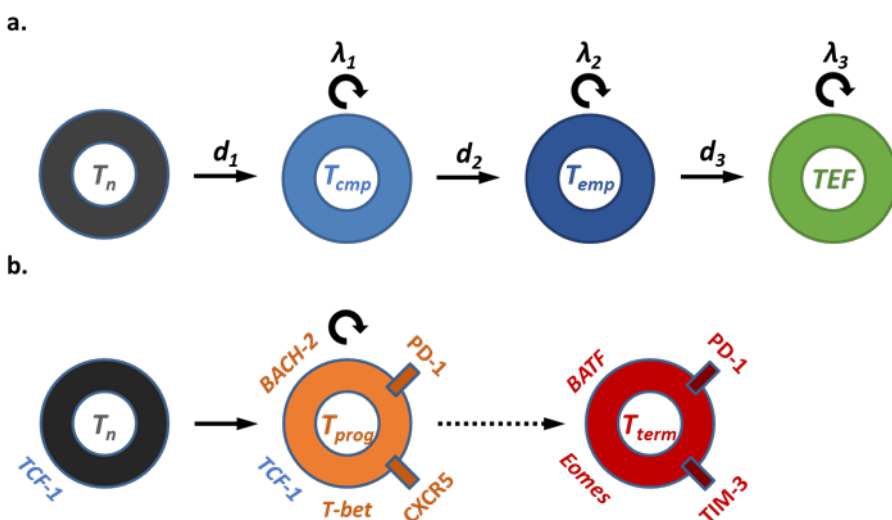


**Figure 3: Developmental framework of early functional and exhausted  $CD8^+$  T cell responses. a-b.**

**a.** Prediction from single cell analyses for  $CD8^+$  T cell diversification in acute infection (modified from Buchholz et al., 2013)  
**b.** Graphical abstract summarizing current models of  $T_{ex}$  development (modified after McLane et al., 2021; Beltra et al., 2020; Utzschneider et al., 2020; Chen et al., 2019; Yao et al., 2019; Utzschneider et al., 2016b; Paley et al., 2012)

Exhaustion is generally thought of to happen relatively soon along a T-cells diversification trajectory, and- following recent observations - to originate within the TCF-1<sup>+</sup>precursors, which subsequently pass it on to the more differentiated populations (Utzschneider et al., 2020; Tsui et al., 2022).

### **1.5. *Lymphocytic choriomeningitis virus* in immunological studies**

*Lymphocytic choriomeningitis virus* belongs to the of *Arenaviridae* family, genus *Mammarenavirus*. It is enveloped, and its single-stranded RNA genome bisegmented into a short (S) and long (L) ambisense segments, encoding nucleoproteins (NPs, especially NP396 and NP276) and glycoproteins (GPs, especially GP33-41), representing the main immunodominant epitopes, a zinc-binding protein (Z-protein) and the viral RNA-Polymerase. Rodents, chiefly mice, are its principal host (Rollin et al., 2015; Vilibic-Cavlek et al., 2021). Muckenfuss, Armstrong and Webster first isolated it while investigating the source of an outbreak of encephalitis in St. Louis in 1933 (Muckenfuss et al., 1934), which was later discovered to have been caused by a flavivirus, which was then termed St. Louis encephalitis virus as a reference to this epidemic (Zhou et al., 2012). Other early studies were performed in the laboratory of Erich Traub at Princeton at a similar time (Traub, 1935).

LCMV is non-cytopathic (Ciurea et al., 1999), and thus histological changes and clinical manifestations are a consequence of CTL-mediated cytotoxicity (Cole et al., 1972). The virus is a potential zoonosis, transmitted by aerosols of infected bodily fluids from mice to humans (Vilibic-Cavlek et al., 2021). Different statistics have been published regarding seroprevalence, with a study among a population in southern Spain listing 1,7% of humans and 9% of mice as having specific antibodies (Lledó et al., 2003). Most infected individuals present no or mild flu-like symptoms after an incubation period of one to three weeks (Bonthius, 2012). Percutaneous exposure, typically occupational needle-stick injuries with contaminated material among laboratory personnel, has been reported to result in aseptic meningoencephalitis in healthy adults, remitting completely without neurological residues within weeks (Aebischer et al., 2016). Still, fatal disease has occurred in immunocompromised patients (Fischer et al., 2006) and the virus has also been identified as a potential teratogen (Jamieson et al., 2006).

Multiple strains of LCMV exist, differing in the kinetics of the infection they cause. LCMV Armstrong – named for its discoverer, Charles Armstrong – induces an acute response and is rapidly cleared from the blood even before the peak of the effector phase at seven to eight days post infection due to CD8<sup>+</sup> T cell activity (Jamieson et al., 1987; Anderson et al., 1985; Mims & Blanden, 1972). LCMV Clone 13 results in a chronic, exhaustive infection with two to three months of viremia in immunocompetent mice, after which virus persists in some tissues such as brain and kidney (Wherry et al., 2003; Ahmed et al., 1984; Matloubian et al., 1990; Matloubian et al., 1993). In the absence of antigen-specific CD4<sup>+</sup> T cell help, hosts remain viremic for life (Matloubian et al., 1994). These strains differ by two amino acids; both mutations contribute to Clone 13's ability to persist in the host (Matloubian et al., 1993). One affects the viral RNA-polymerase and results in increased replicative capacity (Bergthaler et al., 2010), the other increases affinity for the cellular receptor  $\alpha$ -Dystroglycan and leads to changes cell tropism and increased infection of macrophages found in the splenic white pulp (Smelt et al., 2001), as opposed to the neurotropic Armstrong (Vilibic-Cavlek et al., 2021).

Knowledge and availability of a variety of immunodominant epitopes (van der Most et al., 1998; Gairin et al., 1995) and the opportunity to directly compare immune responses of divergent kinetics directed at them in addition to the profound understanding of mouse immunology and genetics, have established LCMV as valuable model system. Its implementation has facilitated great advancements in our concept CD8<sup>+</sup> T cell biology. In addition to viral persistence, key discoveries relating to immunosuppression and exhaustion (Zajac et al., 1998; Ciurea et al., 1999; Traub, 1936; Wherry et al., 2007; Oldstone et al., 1973), MHC-restriction (Zinkernagel & Doherty, 1974), memory formation (Sallusto et al., 1999; Lau et al., 1994), perforin and its relevance for CTL-mediated cytotoxicity (Kägi et al., 1994; Masson & Tschopp, 1985), immunopathology (Cole et al., 1972; Gilden et al., 1972), tolerance (Volkert et al., 1975) and autoimmunity (Oldstone et al., 1991; Ohashi et al., 1991; Pfizenmaier et al., 1975) were made utilizing LCMV.

### **1.6. Single cell *in vivo* fate mapping as a tool to determine lineage relationships**

As the most basic constituent of a cellular immune response, a single naïve CD8<sup>+</sup> T cell will give rise to progeny adopting all phenotypes represented in the overall CTL population in

that specific context. The “One cell, multiple fates” concept (Reiner et al., 2007) (*Figure 4a*) was validated by the recovery of memory and effector subsets after true single cell adoptive transfer of naïve, congenically marked OT-I T cells in the context of an acute bacterial infection with *L.m.*-OVA (Stemberger et al., 2007) and following intrathymic injection of naïve, barcoded transduced OT-I thymocytes (Gerlach et al., 2010).

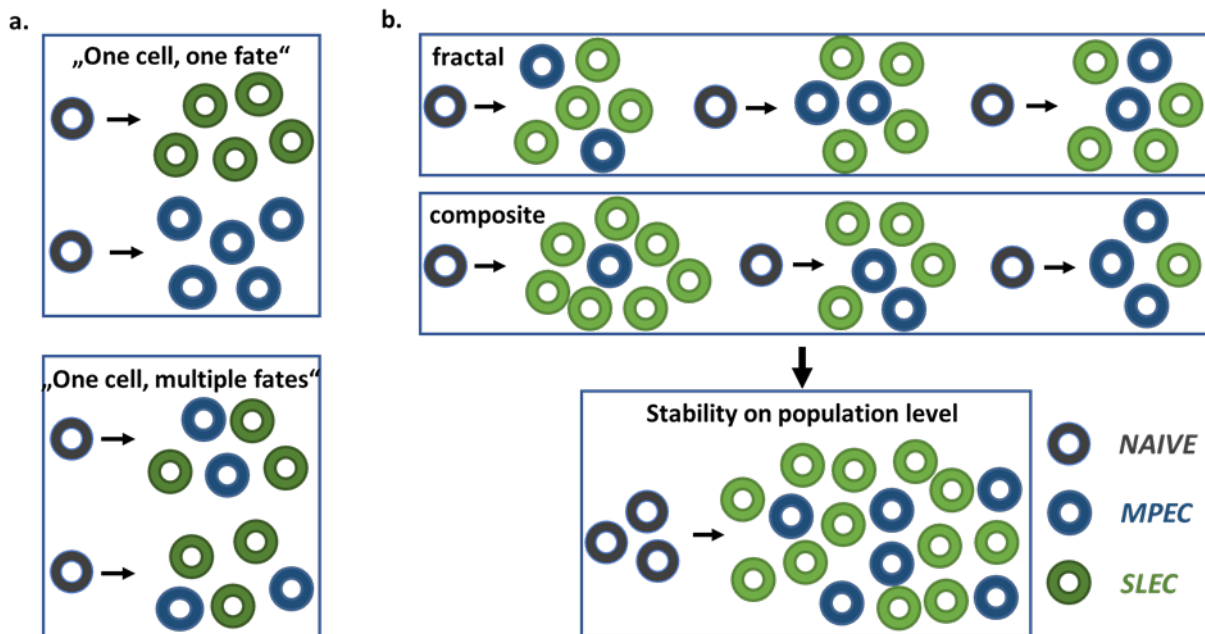


**Figure 4: Relation between single cell- and population-derived CD8<sup>+</sup> T cell responses. a-b.**

**a.** Generation of heterogeneous CD8<sup>+</sup> T cell responses by clones of uniform („one cell, one fate“) or diverse phenotype („one cell, multiple fates“)

**b.** Single cell clones could constitute reproducible responses on the population level in either a fractal or composite fashion (modified from Buchholz et al., 2016)

Hypotheses about the factors prompting heterogeneity of cell fate give varying degrees of emphasis to initial priming as cell-intrinsic and inflammatory cues as cell-extrinsic stimuli and include (Buchholz et al., 2016): asymmetric cell division induced by prolonged interaction between lymphocyte and DC (Chang John et al., 2007); the decreasing potential model (*Figure 5b*), in which accumulation of signals diminishes memory potential (Ahmed & Gray, 1996); the model of linear differentiation (*Figure 5c*) of effectors into memory cells (Opferman et al., 1999); and the progressive differentiation model, which correlates the strength of the priming signal with effector differentiation (*Figure 5a*) (Lanzavecchia & Sallusto, 2000).

Two independent studies showed the remarkable variability of single cell-derived responses in terms of proliferative output and phenotype which yields reproducibility on the population level in a composite manner (Buchholz et al., 2013; Gerlach et al., 2013). The

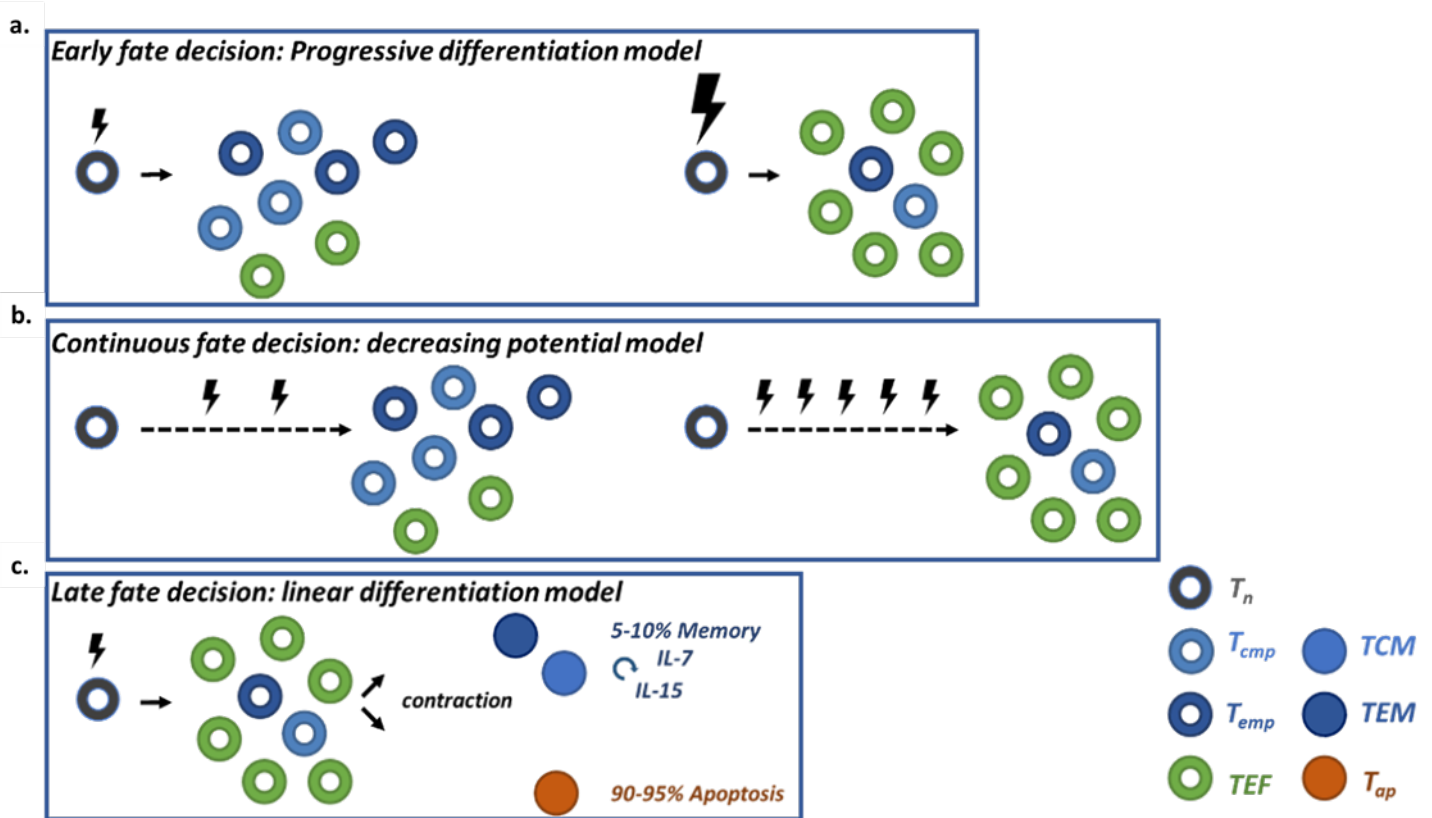


**Figure 5: Models of CD8<sup>+</sup> T cell diversification. a-c.**

**a.** The progressive differentiation model puts emphasis on the strength of the initial TCR stimulus as the main determinant of T cell fate. Strong signals are said to promote effector development, while weaker stimuli lead to a predominant memory phenotype.

**b.** The decreasing potential model views effector and memory fates as the result of a cumulative high or low amount of signals, respectively, received after priming.

**c.** According to the linear differentiation model, the decision to go into apoptosis or adopt memory fate falls at the beginning of contraction. (modified from Buchholz et al., 2016; Ahmed et al., 1996)

required input for robustness was estimated at about 50 for transgenic OT-I T cells.

Furthermore, they revealed a strong positive correlation between burst size and effector phenotype.

Combinations of congenic surface markers (Buchholz et al., 2013), genetic barcodes (Gerlach et al., 2010) or cell-intrinsic, genetically encoded expression of fluorescence proteins (Weber et al., 2011) create unique, heritable labels that allow clonal cell tracing. As the power of single cell fate mapping lies with its ability to separate proliferation and differentiation by ensuing biomathematical analysis, it is especially useful at early phases of the immune response when both processes occur simultaneously at rapid rates and thus facilitating the determination of lineage relationships. In the context of *L.m.* infection, it has supported a linear differentiation pathway from naïve to TCMp, to TEMp and on to TEF, accompanied by an increase in division speed. Applied to chronic infection, it could provide useful insights

## Introduction

---

into the dynamics between subsets of exhausted CD8<sup>+</sup> T cells and their relationship to classical effector and memory T cell subsets, which previously have only been investigated on the population level.

## 2. Aim of this thesis

Continuous antigenic stimulation, as encountered by the immune system in the context of chronic infection causes CD8<sup>+</sup> T cells to adopt a hypofunctional state distinct from that found in an acute setting, which is commonly referred to as “exhaustion” (Zajac et al., 1998). Exhausted cells are characterized by reduced cytotoxic properties, stable expression of potentially multiple coinhibitory receptors, a distinct genetic program significantly impacted by the transcription factor TOX (Alfei et al., 2019) as well as metabolic impairments (Shin & Wherry, 2007). Another important characteristic of exhausted T cell responses is the defect in generating terminally differentiated Short-lived Effector Cells (SLECs) (Henning et al., 2018), which would possibly cause severe immunopathology due to their strong cytolytic activity (Speiser et al., 2014). Both developmental pathways appear to diverge very early after infection, but the precise circumstances of this separation are hitherto unclear. One hypothesis states that signs of exhaustion can first be detected within the *TCF-7<sup>+</sup>* progenitors and move on through the downstream compartments from thereon (Utzschneider et al., 2020). However, these assumptions are based on population-derived studies. The tracking of individual fates can give new insights into the lineage relationships between the distinct subsets of CD8<sup>+</sup> T cells present during the initial stages of exhaustion, which hold relevance for the design of immunological treatments such as checkpoint inhibitor therapy.

More precisely, the goals of this project were:

- to establish single cell fate mapping within the LCMV-system.
- to elucidate the framework of CD8<sup>+</sup> T cell diversification during early exhaustion employing data from single cell fate mapping and sc-RNA-seq analyses.
- to explore the fate of TCF7<sup>+</sup> and TCF7<sup>-</sup> T-cells at the beginning of chronic infection, as well as their distinct functional and developmental capabilities.
- to investigate the development and function of terminally differentiated, KLRG-1<sup>+</sup> effector cells upon exposure to a chronic infection environment.

### 3. Materials and Methods

#### 3.1. Materials

##### 3.1.1. Chemicals and Reagents

REAGENT	SUPPLIER
Ammonium Chloride (NH <sub>4</sub> Cl)	Sigma, Taufkirchen, Germany
Ampicillin Sodium Salt	Carl Roth®, Karlsruhe, Germany
Bovine serum albumin (BSA)	Sigma, Taufkirchen, Germany
BD Cytofix/Cytoperm™ Fixation/permeabilization kit	BD Biosciences, Heidelberg, Germany
Citric acid	Carl Roth®, Karlsruhe, Germany
Disodium phosphate	Carl Roth®, Karlsruhe, Germany
DMEM	Gibco BRL, Karlsruhe, Germany
MEM	Gibco BRL, Karlsruhe, Germany
eBioscience™ Fixable Viability Dye eFlour™ 780	BD Biosciences, Heidelberg, Germany
eBioscience™ FoxP3/Transcription factor staining buffer kit	BD Biosciences, Heidelberg, Germany
Ethanol	Klinikum Rechts der Isar, Munich, Germany
Ethidiummonoazide-bromide	Molecular probes, Leiden, Netherlands
EDTA	Carl Roth®, Karlsruhe, Germany
Fetal calf serum	Biochrome, Berlin, Germany
Formaldehyde 3,5%-3,7%	Otto Fische, Saarbrücken, Germany
Gentamycin	Gibco BRL, Karlsruhe, Germany
L-Glutamine	Sigma, Taufkirchen, Germany
Hanks balanced salt solution (HBSS)	Sigma, Taufkirchen, Germany
Heparin-sodium	Ratiopharm, Ulm, Germany
HEPES	Carl Roth®, Karlsruhe, Germany
Hydrochloric acid (HCl <sub>aq</sub> )	Carl Roth®, Karlsruhe, Germany
Hydrogenperoxide	Carl Roth®, Karlsruhe, Germany
L-Glutamine	Carl Roth®, Karlsruhe, Germany
Methylcellulose	Sigma, Taufkirchen, Germany
OPD	Gibco BRL, Karlsruhe, Germany
Paraformaldehyde (PFA)	Sigma, Taufkirchen, Germany

Penicillin	Carl Roth®, Karlsruhe, Germany
Phosphate buffered saline	Thermo Fisher, Darmstadt, Germany
Propium-iodide	Invitrogen, Carlsbad, USA
RPMI 1640	Thermo Fisher, Darmstadt, Germany
Sodium Chloride (NaCl)	Sigma, Taufkirchen, Germany
Streptomycin	Sigma, Taufkirchen, Germany
Tris-Hydrochloride (Tris-HCl)	Carl Roth®, Karlsruhe, Germany
Triton X	Carl Roth®, Karlsruhe, Germany
Trypan Blue solution	Sigma, Taufkirchen, Germany
Zombie UV™ Fixable Viability kit	Biolegend, San Diego, USA

### 3.1.2. Buffers and Media

<b>BUFFER</b>	<b>COMPOSITION</b>
Ammonium chloride-Tris (ACT)	0.17 M NH <sub>4</sub> Cl 0.3 M Tris-HCl, pH 7.5
FACS buffer, pH 7.45	1x PBS 0.5% (v/w) BSA 1.65% (v/v) NaN <sub>3</sub>
RPMI 10+ cell culture medium	RPMI 1640 10% (v/v) FCS 5% (v/v) SC+
SC+ (medium supplement)	1ml β-Mercaptoethanol 20ml Gentamycin 23,83g HEPES 4g L-Glutamin 200ml Penicillin/Streptomycin
DMEM 10+ cell culture medium	DMEM 10% (v/v) FCS 5% (v/v) SC+
MEM	

**3.1.3. Antibodies**

<b>ANTIBODY</b>	<b>CLONE</b>	<b>SUPPLIER</b>
$\alpha$ -APC-Biotin		
$\alpha$ -CD4 APCCy7	GK1.5	Biolegend, San Diego, USA
$\alpha$ -CD4 PE Dazzle 594	RM4-5	Biolegend, San Diego, USA
$\alpha$ -CD8a FITC	53-6.7	Biolegend, San Diego, USA
$\alpha$ -CD8a Pacific Blue	53-6.7	Biolegend, San Diego, USA
$\alpha$ -CD8a Pacific Orange	5H10	Thermo Fisher, Darmstadt, Germany
$\alpha$ -CD16/32 (FC $\gamma$ -RII/III; Fc-Block)	2.4G2	BD-Biosciences, Heidelberg, Germany
$\alpha$ -CD19 APCCy7	6D5	Biolegend, San Diego, USA
$\alpha$ -CD19 PE-CD594	1D3	BD-Biosciences, Heidelberg, Germany
$\alpha$ -CD25 APC	PC61.5	Thermo Fisher, Darmstadt, Germany
$\alpha$ -CD44 FITC	IM7	Biolegend, San Diego, USA
$\alpha$ -CD45.1 APC	A20	Biolegend, San Diego, USA
$\alpha$ -CD45.1 FITC	A20	Biolegend, San Diego, USA
$\alpha$ -CD45.1 Pacific Blue	A20	Biolegend, San Diego, USA
$\alpha$ -CD45.1 PE	A20	Biolegend, San Diego, USA
$\alpha$ -CD45.1 PE Dazzle 594	A20	Biolegend, San Diego, USA
$\alpha$ -CD45.1 PECy7	A20	Biolegend, San Diego, USA
$\alpha$ -CD45.2 Brilliant Violet 421™	104	Biolegend, San Diego, USA
$\alpha$ -CD45.2 Brilliant Violet 650™	104	Biolegend, San Diego, USA
$\alpha$ -CD90.1 APC	HIS51	Thermo Fisher, Darmstadt, Germany
$\alpha$ -CD90.1 FITC	HIS51	Thermo Fisher, Darmstadt, Germany
$\alpha$ -CD90.1 Pacific Blue	HIS51	Thermo Fisher, Darmstadt, Germany
CD90.2 APC-eFlour 780	53-2.1	Thermo Fisher, Darmstadt, Germany
$\alpha$ -CD90.2 Brilliant Violet 650™	30-H12	Biolegend, San Diego, USA
$\alpha$ -CX3CR1 PECy7	SAO11F11	Biolegend, San Diego, USA
$\alpha$ -CXCR5 PE	SPRCL5	Thermo Fisher, Darmstadt, Germany
$\alpha$ -CXCR5 APC	SPCL5	Thermo Fisher, Darmstadt, Germany
$\alpha$ -IL2 Brilliant Violet 421™	JES6-5H5	Biolegend, San Diego, USA
$\alpha$ -IFN- $\gamma$ PECy7	XMG1.2	Biolegend, San Diego, USA

## Materials and Methods

$\alpha$ -KLRG-1 APC	2F1	Biolegend, San Diego, USA
$\alpha$ -KLRG-1 Brilliant Violet 421™	2F1	Biolegend, San Diego, USA
$\alpha$ -KLRG-1 PE	2F1	Biolegend, San Diego, USA
$\alpha$ -Ly108 APC	330-AJ	Biolegend, San Diego, USA
$\alpha$ -PD-1 Brilliant Violet 510™	29F.1A12	Biolegend, San Diego, USA
$\alpha$ -PE-Biotin	PE001	Biolegend, San Diego, USA
$\alpha$ -TCF7 PE	S33-966	BD-Biosciences, Heidelberg, Germany
$\alpha$ -Tim-3 APC	RMT3-23	Biolegend, San Diego, USA
$\alpha$ -Tim-3 Brilliant Violet 421™	RMT3-23	Biolegend, San Diego, USA
$\alpha$ -TNF- $\alpha$ Brilliant Violet 510™	MP6-XT22	Biolegend, San Diego, USA
$\alpha$ -TOX Alexa eFlour 660	TXRX10	Thermo Fisher, Darmstadt, Germany
$\alpha$ -TOX PE	TXRX10	Thermo Fisher, Darmstadt, Germany
<i>InVivo</i> Mab anti-LCMV nucleoprotein	VL-4	Bio X Cell, Lebanon, USA
Peroxidase-conjugated AffiniPure Goat Anti-Rat IgG (H+L)		Jackson ImmunoResearch Laboratories Inc, West Grove, USA
Streptavidin APC		Biolegend, San Diego, USA
Streptavidin PE		Biolegend, San Diego, USA

### 3.1.4. Equipment

EQUIPMENT	MODEL	SUPPLIER
Biological safety cabinets	HERAsafe™	Heraeus, Hanau, Germany
Cell culture incubator	Heracell™ 240i	Heraeus, Hanau, Germany
Cell sorters	MoFlo XDP	Beckmann Coulter, Fullerton, USA
	MoFlo Astrios	Beckmann Coulter, Fullerton, USA
Centrifuges	Heraus Multifuge™ X3R	Heraeus, Hanau, Germany
Flow Cytometers	CytoFlex LX	Beckmann Coulter, Fullerton, USA
	CytoFlex S	Beckmann Coulter, Fullerton, USA
Microscope	Axiovert S100	Carl Zeiss, Jena, Germany
pH-Meter	MultiCal® pH 526	WTW, Weilheim, Germany
Water Bath	LAUDA Ecoline 019	Lauda, Königshofen, Germany
Weighing Scale	CP 124 S	Sartorius, Göttingen, Germany

### 3.1.5. Software

SOFTWARE	SUPPLIER
FloJo (V10)	Treestar, Ashland, USA
GraphPad Prism (V9.0)	GraphPad Software, LaJolla, USA
Microsoft Office for Windows 10	Microsoft, Redmond, USA

## 3.2. Methods

### 3.2.1. Mice

Routinely, female C57BL/6 mice were acquired from Envigo at an age of six to eight weeks. P14 transgenic Matrix doner mice were bred and kept under SPF conditions. All experimental procedures and animal handling were executed according to the institutional protocol, previously approved by the designated local authorities.

### 3.2.2. Preparation of cell suspensions from different organs

In order to obtain leukocyte suspensions for flowcytometric analysis, whole spleens were strained into 5 cm petri dish prefilled with 5ml RPMI 10+ medium using a cell strainer (either 40 $\mu$ m or 70 $\mu$ m) and the stopper of a 2ml syringe. The content was then transferred to 15ml falcons. Dish and strainer were rinsed with an additional volume of 5ml medium to gather remaining cells, which was then added to the volume in the tube. After six minutes of centrifugation (at 1500 rpm and RT), supernatant was removed and 3ml ACT were added, resulting in lysis of contained erythrocytes. After 3 minutes, the process was stopped by diluting the reagent with a greater volume of cold medium. Following a second centrifugation stop, samples were resuspended in FACS buffer. Appropriate aliquots were mixed with a Trypan blue solution, allowing live-dead discrimination, and manually counted in a Neubauer chamber to determine cell numbers for all samples, which were then diluted to a concentration of 5x10<sup>7</sup> cells per ml.

After preparation, lungs were either fixated in PFA for 48h minimum and given to pathology for histological evaluation, or otherwise prepared for FACS staining. Both lobes were cut into cubes of less than 3mm edge length and incubated in 2ml HBSS buffer at 4°C in falcons for 30min. An half hour of Collagenase digestion at 37°C were preceded and followed by two

washing-steps in RPMI-10+, after which the tissue fragments were transferred into nylon cell strainers in petri dishes using and from then on treated as described previously for spleens. Livers were strained in RPMI and centrifuged as described above. The resulting cell pellet was resuspended in 3ml 40% Perchol and then underlaid with another 3ml of Perchol in an 80% dilution. 20min density centrifugation at 2600rpm, room temperature and with acceleration and deceleration set to zero produced a clearly distinguishable layer of RBCs also containing the desired lymphocytes, which was carefully collected with a 1000 $\mu$ l pipette, followed by RBC lysis analogous to spleens.

Blood specimens were acquired in 1.5ml Eppendorf tubes filled with 25 $\mu$ l of heparin to prevent clotting. To accommodate the high content of red blood cells, protocol was adapted to include two consecutive lysis steps: at first, ten min incubation in ten ml of ACT, and after centrifugation and removal of the supernatant, addition of another 5ml, this time stopped by addition of an equivalent volume of medium after 5min.

If the material was intended for adoptive cell transfer, preparation and all ensuing steps of the staining protocol were carried out under sterile conditions and using sterile reagents and equipment.

### **3.2.3. Staining protocols for FACS analysis of cell surface antigens**

Staining for FACS-based analysis was predominantly performed in 96-well V-bottom plates. To that purpose, typically  $10^7$  cells were transferred to each well, possibly in duplicates or triplicates depending on the requirements of the specific experiment. Blood samples on average contained about  $10^6$  cells and were stained in their entirety, as was the lymphocyte coat recovered from livers. After preparation of lungs, about 20% of the resulting cell material was processed further. To prevent unspecific binding of the respective antibodies, a 20 min incubation period with  $\alpha$ -CD16/32 at 4°C was performed previously to the surface staining. Different reagents were employed for the discrimination of dead cells. PI was used mostly on cells meant for adoptive transfer and applied after the surface antigens had been stained. Fixable Viability Dye eFlour780™ was either added to the samples simultaneously with the Fc-block, or directly to the surface staining antibody mixture in situations with low probability of unspecific binding. The UV™ Zombie Fixable Viability kit was reconstituted with DMSO according to the manufacturer's instructions and incubated with the cell

material in PBS at a dilution of 1:100 for 20 min at 4°C. After two washing steps with 100µl and 200µl FACS buffer, respectively, followed a 30 min incubation period at 4°C with 100µl of the “mastermix”, containing all antibodies for surface staining at the previously titrated concentration. When staining chemokine receptors, such as CX3CR1 or CXCR5, labelling time was extended to 45 min and performed at RT, allowing for continued physiological recirculation between cell surface and cytoplasm to optimize labelling. To facilitate detection of the rather dim CXCR5 signal, a three-step amplification protocol was employed. After staining with the primary α-CXCR5-PE antibody, first a biotinylated α-PE-antibody was added for 20min at RT and a dilution of 1:100 followed by PE-conjugated Streptavidin (1:200, 45min, RT). Before analysis, samples were washed thrice more, once with 100µl and twice 200µl FACS, to remove all excess antibodies and fixated in a 1% PFA solution to inactivate potentially infectious virus particles. Single stain fluorescence controls were prepared from pooled material from all samples following the same protocol.

#### **3.2.4. Staining protocols for FACS analysis of intracellular antigens**

For the detection of transcription factors, the eBioscience FoxP3/Transcription factor staining buffer set was used according to the manufacturer’s instructions. Live/dead discrimination, Fc-Block and staining of surface antigens was executed as described in 3.2.3, followed by 20 min permeabilization with the Fixation/Permeabilization concentrate (100µl per well at 4°C). The Washing buffer was appropriately diluted and used to wash the samples twice (100µl and 200µl, respectively, centrifuge set at 4°C and 1800rpm). It also served as the basis for antibody mixture for the intracellular staining, which was performed by 45 min of incubation with 100µl at 4°C. Finally, samples were washed three times (100µl, 200 µl and 200µl), each time incubating with the washing buffer for 10min in order to let excess antibody diffuse out of the cells.

#### **3.2.5. Peptide restimulation and measurement of cytokine production**

As a means to evaluate functionality we measured the cells’ ability to produce effector cytokines. For this assay, leukocytes were obtained from spleens as described in 3.2.2. After counting, triplicates of 10<sup>7</sup> cells per sample were transferred to a 12-well cell culture plate and resuspended in a total volume of 2ml RPMI per well. To two of those, 2µg of gp33-peptide were added while the remaining one was left untreated to serve as a negative

control. Five hours of restimulation in the cell culture incubator (37°C, 5% CO<sub>2</sub>) followed, after the first of which 2 µl of BD GolgiPlug™ protein-transport inhibitor (containing Brefeldin A) were carefully pipetted into the top of each well, preventing secretion of the produced cytokines and thus enabling their detection within the respective cell later on. Thereafter, cells were transferred to 15ml falcons, washed twice with fresh medium to remove soluble antigen before transfer into a 96-well V-bottom plate for staining. Initially, surface antigens were stained adhering to the protocol described in 3.2.3. The samples were then resuspended in 100µl of Fixation/Permeabilization solution from the BD Cytotfix/Cytoperm™ Fixation/permeabilization kit and incubated at 4°C in the dark for 30 min. Two washing steps with 100µl and 200µl (centrifuge set at 4°C and 1800rpm) of 1x BD Perm/Wash™ Buffer were performed previously to addition of the anti-cytokine antibodies in the appropriate dilution (also using the buffer supplied in the kit). After a 45 min incubation period (dark, 4°C), three more washing steps (100µl, 200µl and 200µl respectively, each time incubating with the Wash buffer for 5 min) did away with any remaining staining reagents.

### 3.2.6. Flow cytometric cell sorting

For single cell transfer experiments, P14 cells from eight donor mice with distinct congenic phenotypes (P14 “Matrix” with different homo- and heterozygous combinations of CD45.1/2 and CD90.1/2, as reported in Buchholz et. al *Science*, 2013a) were obtained from peripheral blood. Either a MoFlo XDP or MoFlo Astrios (both manufactured by Beckmann Coulter) was used to sort each matrix component (A through H) separately at single cell purity mode for CD8<sup>+</sup>/CD44<sup>-</sup> into the wells of a 96-well V-bottom plate prefilled with 4x10<sup>5</sup> wild-type, unstained splenocytes suspended in 200µl filtered FCS. This process yielded one cell of each component A-G and a count of either 100 or 500 for component H, serving as a population control to assess transfer efficiency and correct onset of infection, per well, the contents of which were, after brief centrifugation at 1500rpm, carefully resuspended and taken up with a syringe to be intraperitoneally injected into the recipients.

When sorting and analyzing entire spleens, we employed a technique developed by our Flow Cytometry Core Facility CyTUM for this particular purpose termed “Speed enrichment”. This entails staining a single antigen, such as a congenic marker, on a channel with a strong and clear fluorescence signal, such as APC or FITC., which is then used as a sorting trigger while running the sample at a high flow rate. Combined with an ensuing secondary sort with a

more discriminatory panel, this greatly potentiates yield per time when isolating rare cell populations.

### **3.2.7. FACS-based analysis**

Data were acquired on a CytoFlex LX or CytoFlex S (both products of Beckmann-Coulter) using the manufacturer's original operating system. Larger clots of cell material were removed by filtration through a nylon mesh. The resulting cell counts generally varied between  $1-2 \times 10^7$  per sample. Treestar's FloJo software was used for data analysis.

### **3.2.8. Viruses and infections**

Mice were injected with either  $2 \times 10^5$  PFU LCMV-Armstrong intraperitoneally or  $2 \times 10^6$  PFU LCMV-Cl13 intravenously, resulting in an acute or chronic infection. Initially, virus stock was kindly provided by the group of Prof Dr. Dietmar Zehn at the School of Life Sciences in Weihenstephan. According to their protocol, we established its propagation in our own laboratory. The potency of each batch was determined by measuring viral load in the harvested supernatant by plaque assay, allowing for the calculation of the correct dosage to be administered.

### **3.2.9. Cell lines**

P14-TCF-7-GFP reporter cells were also kindly provided to us by the AG Zehn before successful import of this reporter line into our own animal facility, as were frozen Vero (African Green Monkey kidney) cells.

### **3.2.10. Virus propagation and plaque assay**

Virus was propagated by infecting BHK-cells with either LCMV-Armstrong or LCMV-Clone 13, culturing them and collecting the supernatant from the cell culture flask. In order to determine the potency of the resulting stock and thus enable the calculation and administration of the correct dosage, viral titer was measured by plaque assay. This protocol first required growing a culture of Vero cells to a loose confluence of roughly 70% before harvesting them by trypsinization and resuspending them at a concentration of  $8 \times 10^5$ /ml in Minimal Essential Medium supplemented with 5% FCS (MEM-5). The material to be analyzed was prepared by freezing at  $-80^\circ\text{C}$ , releasing the virus particles.  $50 \mu\text{l}$  of a blood sample

would be diluted with 200µl MEM-5, and 100µl of the resulting mixture added to the top well of one row on the plate. Analogously, 200µl of a splenocyte solution could be used. After careful resuspension, 100µl were taken up with a fresh pipet tip and transferred to the well below, yielding a fivefold dilution. This process was repeated four to six times in total, depending on the anticipated viral load. 200µl of the cell suspension were transferred to a new 24-well plate, after which the virus dilution was added - lowest to highest, using the same tip. Following three hours of incubation, the samples were coated with 400µl 1x DMEM-Methylcellulose to inhibit further dispersal of the virus particles, confining them to those cells already infected by this point. After a total of 72 hours in the cell culture incubator (5% CO<sub>2</sub>, 37°C), the supernatant was aspirated and the cells adhering to the bottom of the well were fixated with 400µl 4% PFA for 30 min prior to incubation with 200µl Triton X for 20 min and washing with PBS supplemented with 5% FCS (PBS 5%) before adding the primary α-VDLA-4 antibody (in PBS 2%, 200µl/well). Following another incubation period of one hour and two ensuing washing steps, the secondary α-Peroxidase-antibody was added (200µl/well, PBS 2%) remaining on the samples for another 60 minutes. The appropriate dilution of both antibodies was subject to the varying concentration of the respective lot. After two washing steps, Ortho-Phenyldiamin-hydrochloride (OPD) substrate (consisting of 25ml H<sub>2</sub>O, 12,5 ml of each solution C and D, one tablet OPD and 50µl hydrogenperoxide) was added to the cells, causing a peroxidase reaction detectable as a color shift to black after 15 min in infected cells. Counting the thus emerged “plaques” under consideration of the respective dilution allowed for the calculation of viral titers. The supernatant resulting from the OPD-reaction was separately disposed of as toxic waste.

### **3.2.11. Data visualization and statistics**

Prism 9 (by GraphPad) served as the main tool to generate descriptive statistics, statistical analysis, and data visualization. Routinely, a potential Gaussian distribution of the data was assessed using D'Agostino-Pearson omnibus normality test after which P values were calculated by means of One-way ANOVA, Mann-Whitney-U or Spearman non-parametric tests. Significance levels as indicted: \*P < 0.05, \*\*P<0.01, \*\*\*P<0.001, \*\*\*\*<0.0001.

### **3.2.12. Biomathematical calculation and modelling**

Biomathematical modelling based upon the single cell data was performed by the group of Michael Flossdorf, especially Albulena Toska, at the Institute for Microbiology, Immunology and Hygiene of the Technical University of Munich. This contribution encompassed the generation and analysis of single cell RNA-sequencing data, employing velocities among other techniques. These analyses included previously published an publicly available sc-RNA-seq data obtained from days 4.5 and 8 p.i. of LCMV-Arm and LCMV-Cl13 infection (Chen et al., 2019; Yao et al., 2019). A complementary data set for day 6 p.i. of was generated by harvesting and preparation of splenocytes from mice infected with both virus strains which were sent to 10x Genomics for further processing and sequencing.

## 4. Results

### 4.1. Single cell *in vivo* fate mapping in acute and chronic LCMV infection

#### 4.1.1. Establishing LCMV as a murine model system to study immune responses against acute and chronic infections

In order to determine phenotype and function of cells present in different phases of acute and chronic infection as well as their respective dynamics, we transferred populations of 500 TCR-transgenic P14 cells, recognizing the gp33 epitope of LCMV, intraperitoneally into naïve C57BL/6 recipients, which were infected with standard doses of LCMV Clone 13 or Armstrong ( $2 \times 10^6$  PFU intravenously or  $2 \times 10^5$  PFU intraperitoneally, respectively) 24 hours later (Fig. 6a). At several timepoints over the course of infection, mice were sacrificed, and

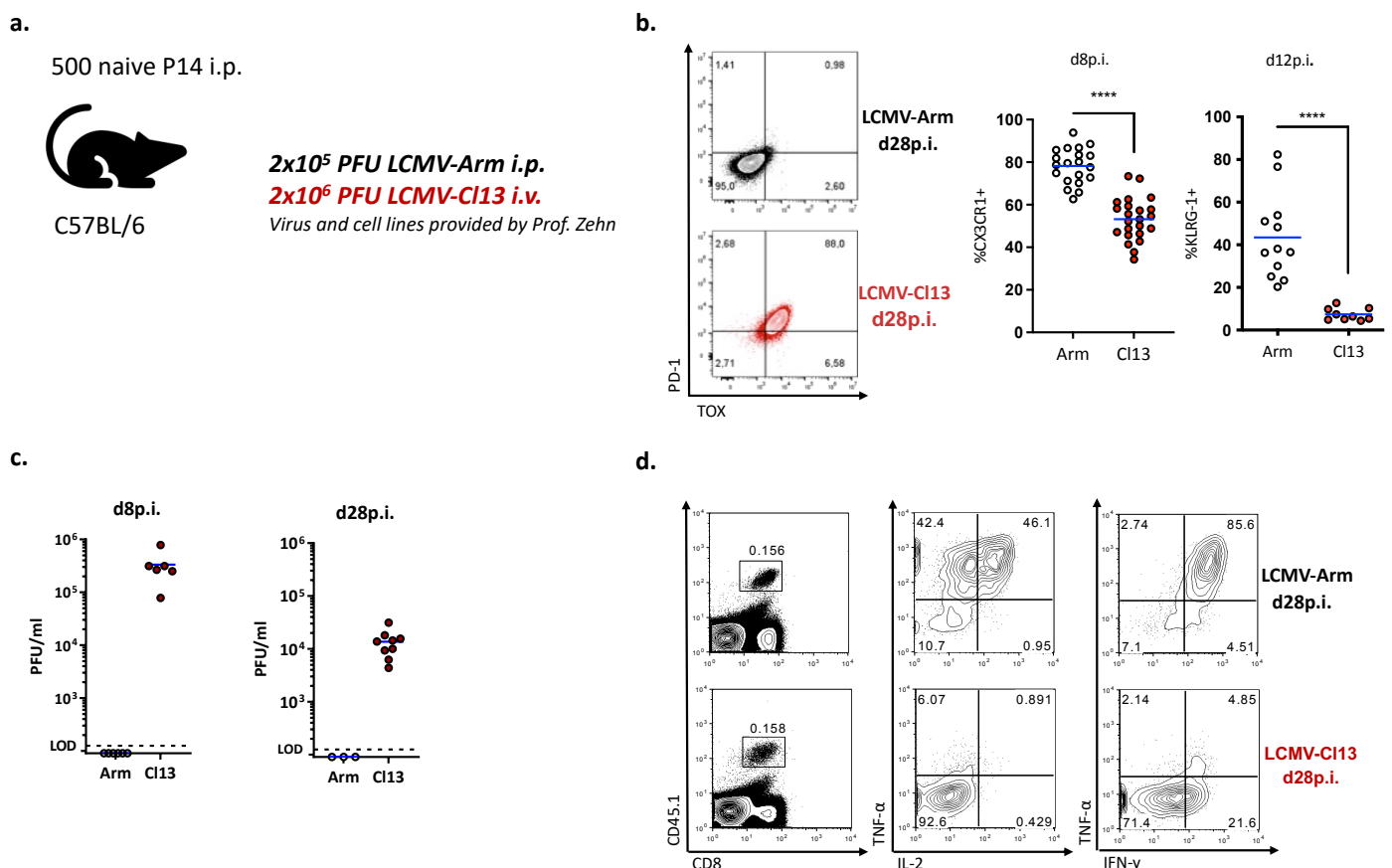


**Figure 6: P14 mount phenotypically distinct responses after acute and chronic LCMV infection. a-d.**

**a.** Vaccination scheme for acute and chronic strains of LCMV.

**b.** Upregulation of typical exhaustion and effector markers in Cl13 as compared to Arm infection.

**c.** Viral loads at different stages of acute and chronic LCMV infection.

**d.** Chronic LCMV infection induces P14 to produce reduced levels of effector cytokines.

Data represent a single (**d**) or are representative for or compiled of at least two independent experiments (**b-c**). (n = 6). Lines indicate mean. \*\*\*\*P < 0.0001, \*\*\*P < 0.001, \*\*P < 0.01, \*P < 0.05 (Mann–Whitney Test)

spleens harvested to be analyzed for phenotypic markers by flow cytometry. This also served to validate this newly established system in our lab.

At day twelve post infection, a significant amount of cells recovered from the spleens of acutely infected mice stained positive for the killer cell lectin-like receptor G1 (KLRG-1), an early indicator of SLEC fate associated with senescence and terminal differentiation (Joshi et al., 2007); the chemokine receptor CX3CR1, also indicative of cytotoxic potential (Böttcher et al., 2015; Gerlach et al., 2016), could be detected as early as day eight in this setting (*Figure 6b*). Expression of PD-1 was initially prominent as well. This inhibitory receptor is induced in a NFAT-dependent manner upon antigen-recognition (Oestreich et al., 2008) and co-locates to the TCR, forming microclusters and inhibiting the phosphorylation of proximal TCR-signaling molecules (Yokosuka et al., 2012), thus preventing overshooting activation (Okazaki et al., 2013). Both findings correspond to this timepoint reflecting the peak of the immune response, characterized by high numbers of strongly activated effectors (Wherry et al., 2003). Such a population failed to emerge even by day 28 p.i. of the Cl13 infection, while PD-1 was maintained at significant levels as opposed to its transient upregulation in Armstrong (*Figure 6b*).

Another distinctive feature of cells continuously exposed to antigen is a remodeling of their transcriptional circuitry around the master regulator thymocyte selection-associated high mobility group box (TOX), which is essential for establishing the exhaustion program and long-term maintenance of an immune response against a persisting agent. (Alfei et al., 2019; Khan et al., 2019). Consistently, in the chronically but not the acutely infected host, P14 T cells were predominantly marked from day eight on by stable high expression of this transcription factor (*Figure 6b*). As stated above, viremia in LCMV-Arm is terminated about a week after infection while continuing for months in LCMV-Cl13, with ensuing persistence in some organs (Wherry et al., 2003; Ahmed et al., 1984; Matloubian et al., 1990; Matloubian et al., 1993). As expected, when determining viral load from the blood, titers were still high after four weeks of Cl13 infection, while already below limit of detection at day eight of Armstrong infection (*Figure 6c*).

Chronic infection leads to impaired effector functions, most readily assessed as decreased capacity to produce effector cytokines upon restimulation with cognate peptide (Wherry et al., 2003). We tested cytokine production of antigen-specific P14 T cells, after incubation with their cognate gp33 peptide and found that, compared with classical memory cells

derived from an acutely resolved Armstrong infection, cells recovered from the chronic phase of CI13 indeed proved functionally inferior (*Figure 6d.*). Collectively, these results validated the establishment of the LCMV-system in our laboratory.

#### 4.1.2. Identifying distinct subsets of exhausted CD8<sup>+</sup> T cells

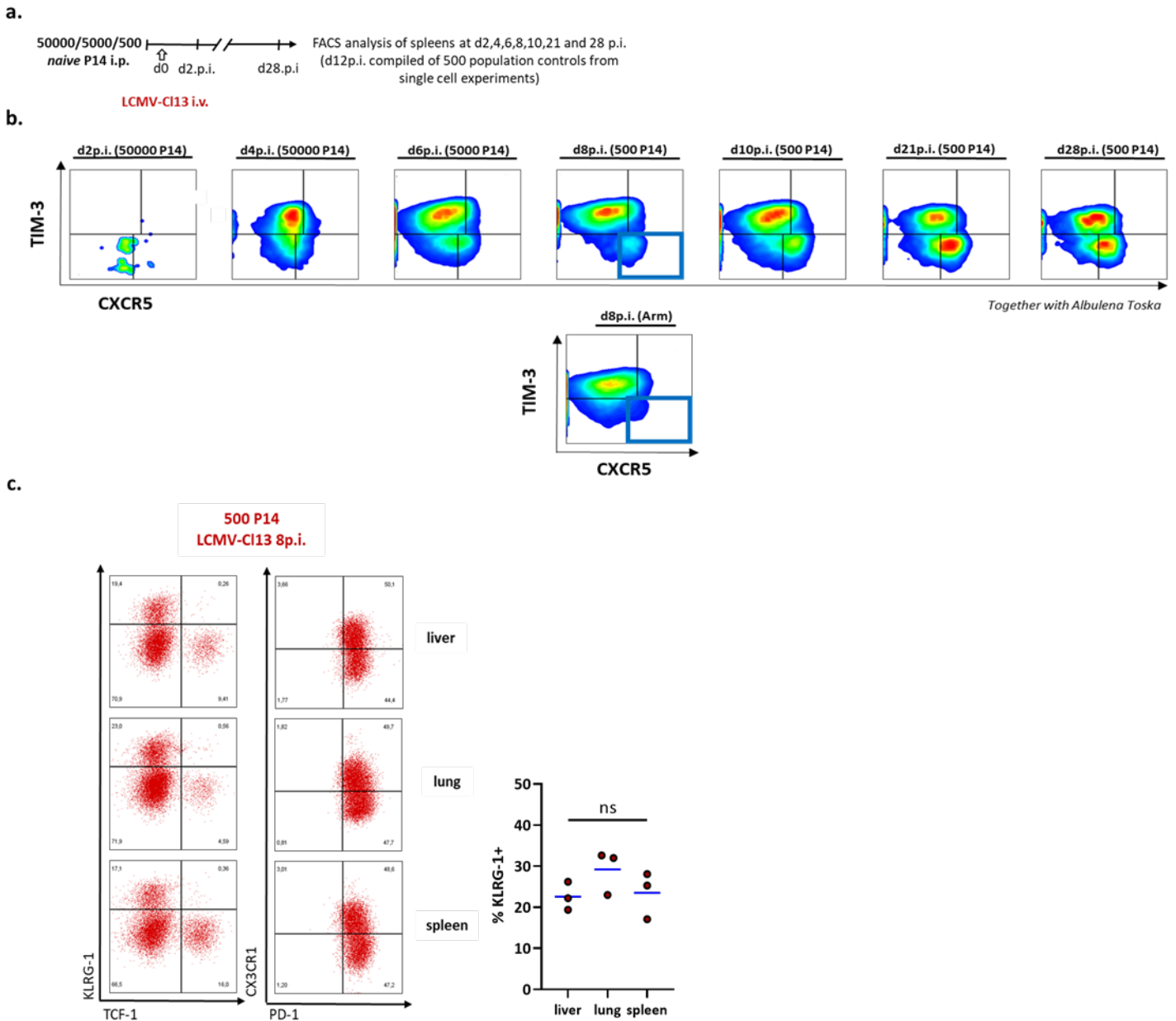


**Figure 7: The first week of LCMV infection sees the development of phenotypically diverse CTL subsets. a-c.**

**a.** Experimental scheme of population kinetic analysis.

**b.** Subsets of precursors and their more terminally differentiated progeny emerge within the first week of LCMV infection. The progenitors are more prominent in the chronic setting.

**c.** Phenotype of P14 recovered across different organs in chronic infection.

Data are compiled out of two independent (**b**) or representative of a single experiment (**c**) (n= 3, **b**: per timepoint). Lines indicate mean. \*\*\*P < 0.0001, \*\*P < 0.001, \*P < 0.01, \*P < 0.05 (Mann-Whitney Test)

In order to assess the population dynamics of CD8<sup>+</sup> T cells in chronic infection, we once more performed population transfers of naïve P14 followed by analysis at consecutive timepoints (*Figure 7a*). These showed the first week of chronic infection to see the emergence of a population positive for CXCR5 and TCF-1, both associated with progenitor fate and long-term maintenance of the response, that constituted an increasingly larger proportion of the immune response over the first four weeks and failed to develop in the acute setting, as previously described (*Figure 7b*). This population of CXCR5 expressing cells was further detected more prominently in the spleen than in the liver or lung (*Figure 7c*).

In-depth spleen analysis performed at day 8 p.i. (*Figure 8a*) in which we stained some of the established markers of distinct fates during chronic infection in combination with well-established indicators of memory and effector differentiation allowed for further characterization of these subsets (*Figure 8b*). Both CXCR5 and TCF1, in combination with either TIM-3 or CX3CR1, identified a second population, which in contrast showed a decreased frequency over time and was slightly more dominant in effector organs such as lung and liver (*Figure 7c*). MFI of TIM-3 was higher after CI13 than Arm infection. Prior to the contraction phase in LCMV-Arm infected mice many cells expressed CX3CR1, with those of particularly high MFI also staining positive for KLRG-1. This is consistent with CX3CR1 more finely delineating the degree of effector differentiation (Gerlach et al., 2016) (*Figure 8b*). As in our previous experiments, P14 T cells did not generate a significant KLRG-1<sup>+</sup>, terminally differentiated population when challenged with CI13, conforming to the understanding of T cell exhaustion as a block on terminal differentiation. More in-depth phenotyping on the level of subsets defined by TIM-3 and Ly108 confirmed the Ly108<sup>+</sup>, hereafter referred to as MPs (memory precursors) population to exhibit memory-associated markers such as TCF-1 and CD27. Ly108<sup>-</sup> cells in LCMV-Arm could be further subdivided into a CX3CR1<sup>high</sup> population strongly enriched for effector molecules such as KLRG-1 and simultaneous expression of Granzyme A and B, and a CX3CR1<sup>low</sup> population characterized by intermediate levels of Granzyme B, which was also present in CI13. While all cells from the chronic setting showed similar levels of PD-1, this coinhibitory receptor was anticorrelated with the degree of effector differentiation in the acute infection, in accordance with past findings showing PD-1 to be repressed in effector cells via Blimp-1 (Lu et al., 2014). Taken together, we identified three main CTL subpopulations present in acute and chronic infection: Memory Precursors (MPs), characterized by TCF-1 and absence of both CX3CR1 and KLRG-1, TCF-1<sup>-</sup> Early

## Results

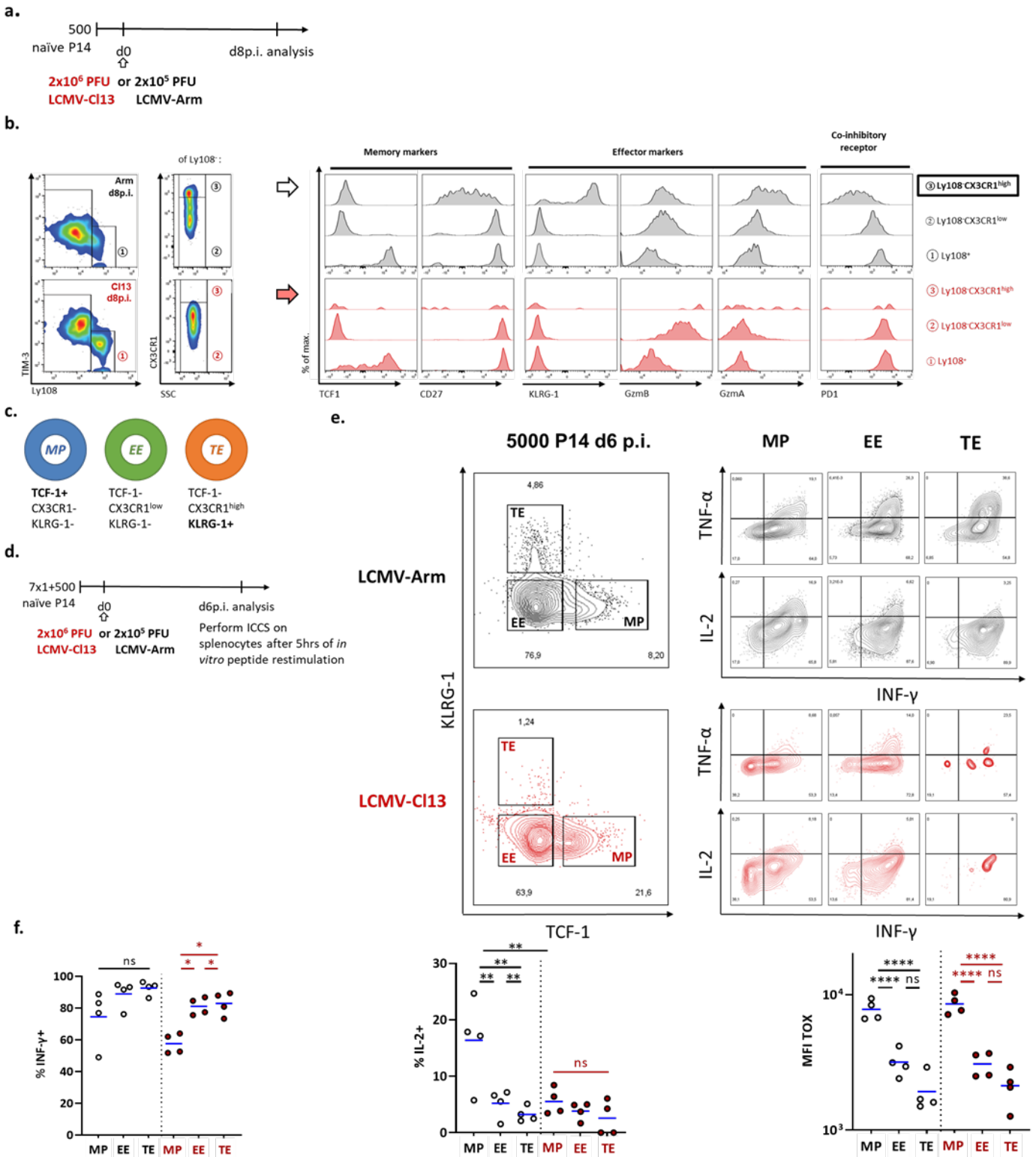


**Figure 8: Expression of CX3CR1 and TCF1 delineates three functionally distinct subsets of CD8<sup>+</sup> T cells. a.-f.**

**a.** Experimental setup of subset phenotyping experiment.

**b.** Distinct population of P14, identified by Ly108, TIM-3 and CX3CR1 express different levels of effector, memory and exhaustion markers.

**c.** TCF-1<sup>+</sup> MPs, CX3CR1<sup>low</sup> EEs and KLRG-1<sup>+</sup> TEs comprise the initial gp33-specific CD8<sup>+</sup> T cell response.

**d.** Experimental setup of functional assessment.

**e.** Functional impairment in Cl13 manifests by day six.

**f.** Reduced production of IL-2 is the first step in the hierarchical loss off effector cytokines.

Data are representative of a single (**b**) or of one out of two independent experiments (**e,f**) (n=3 per group). Lines indicate mean.

\*\*\*\*P < 0.0001, \*\*\*P < 0.001, \*\*P < 0.01, \*P < 0.05 (ANOVA)

Effectors (EEs) expressing low levels of CX3CR1 and Terminal Effector (TEs) distinguished high levels of both CX3CR1 and KLRG-1, which are absent during chronic infection (*Figure 8c*). Functional differences assessed by measuring cytokine secretion and TOX expression were discernible as early as day six p.i., beginning with reduced IL-2 expression by MPs (*Figures 8d-f*).

#### 4.1.3. Single cell *in vivo* fate mapping in acute and chronic infection

Having identified subsets of exhausted and functional CD8<sup>+</sup> T cells on population derived responses, we were interested in investigating their development on the single-cell level. To achieve efficient single-cell transfer, we crossbred transgenic P14 mice with mice carrying the congenic markers CD45.1/2 or CD90.1/2. After several rounds of breeding, this approach yielded a P14 congenic matrix with eight components (A-H) expressing the transgenic TCR and the congenic markers in different combinations of homo- or heterozygosity, and thus

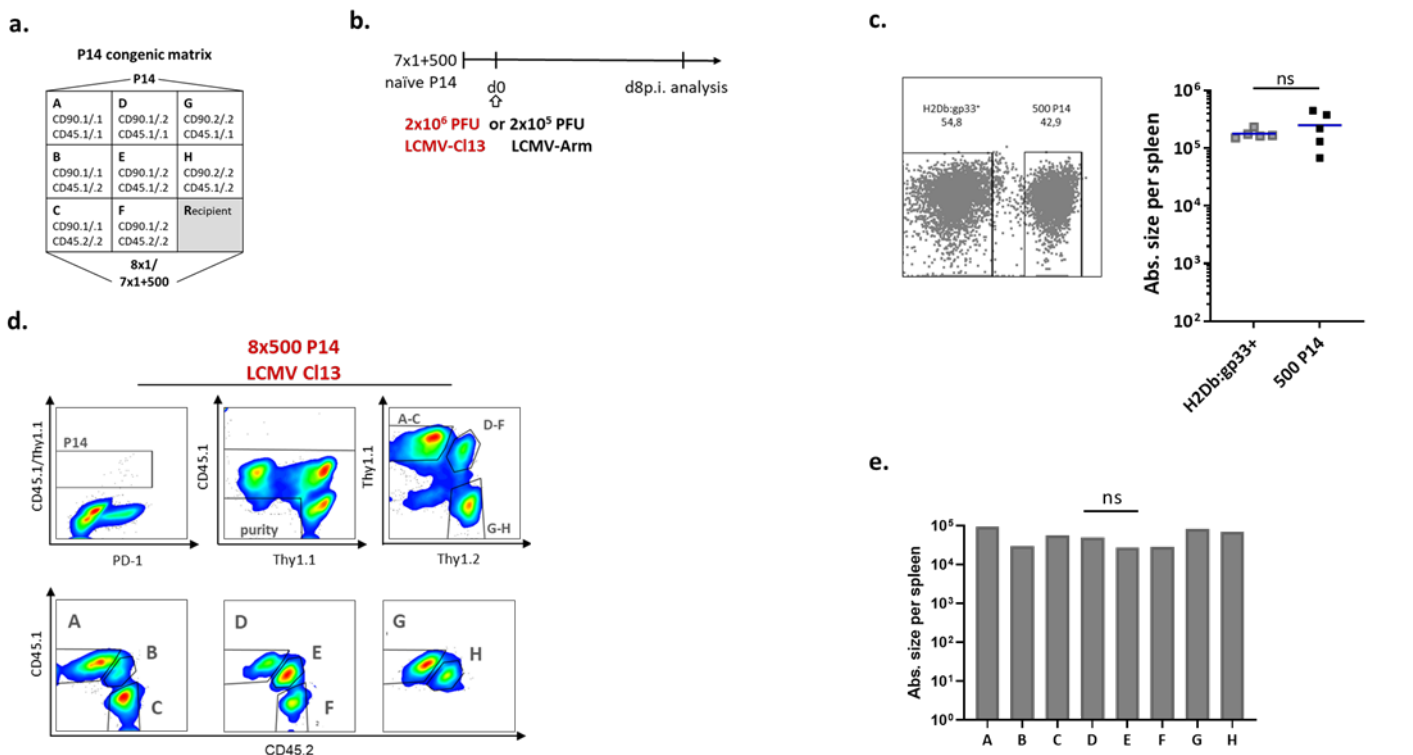


**Figure 9: Single cell *in vivo* fate mapping in acute and chronic LCMV infection. a-e.**

**a.** Scheme of the P14 congenic matrix as heritable tag for tracing individual cell (Buchholz et al, 2013).

**b.** Experimental setup of single cell transfer experiments.

**c.** 500 P14-derived responses mirror that the endogenous H2Db:gp33-specific population in size.

**d.** Exemplary application of the adapted Cytoflex matrix staining panel to a spleen sample from d8p.i. of Cl13 infection following transfer of 8x500 P14 populations.

**e.** Components A-H are each recovered at comparable numbers (Arm d8p.i.).

Data are compiled (**d**) of four (n=1; 8x500 population controls) or representative for one of two independent experiments (**e**)

(**e**: n=5 or 3). Lines indicate mean. \*P < 0.05 (ANOVA (**d**) or Mann Whitney Test (**e**)).

being distinguishable from one another and the host (CD45.2/2, CD90.2/2) (*Figure 9a*).

Seven single naïve P14 cells (A-G) were transferred alongside a population control of 500 naïve P14 cells (H) in order to monitor the average response patterns of T cell populations responding to the infection (*Figure 9b*). We fixed the amount of cells used as controls to mirror that of the endogenous naïve gp33<sup>+</sup> precursors, according to the literature (Jenkins & Moon, 2012; Blattman et al., 2002). Multimer staining for the endogenous compared to the P14- derived response verified similar magnitude of both populations after a transfer of 500 cells (*Figure 9c*).

The staining panel successfully employed in our lab for analyzing single cell experiments in the *L.m.* infection setting at our CyAn flow cytometers did not allow sufficient matrix discrimination in LCMV-infection. Strong antigenic stimuli have been linked to subsequent downregulation of not only the TCR but also CD8 and other associated molecules, among those also congenic markers (DiSanto et al., 1989; Altin & Sloan, 1997; Haeryfar & Hoskin, 2004; Valitutti et al., 1995; Valitutti et al., 1996; Luton et al., 1994; Cantrell et al., 1985; Dietrich et al., 1996). Since gp33 represents a high-affinity ligand for the transgenic P14 TCR (K<sub>D</sub> 3,5μM as compared to 6,5 μM for SIINFEKL: OT-I) (Hommel & Hodgkin, 2007; Boulter et al., 2007), we considered this to be a contributing factor. Consequently, we titrated a new matrix panel adapted for use on the CytoFlex cytometers. This nearly quadrupled the time required for analysis due to the lower capacity of events to be recorded per second (40000 eps vs. 10000 eps) but gave the major advantages of superior sensitivity in detection as well as additional channels and a higher number of separate lasers to excite the fluorophores, minimizing spillover in this delicately balanced panel (*Figure 9d*). As a further validation, all congenic matrix components (A-H) were recovered at comparable numbers after 8x500 population transfer (*Figure 9e*).

Comparative analysis of spleen samples during the early phase of both infections showed phenotypical stability on the population level, while responses derived from single cells exhibited considerable variability, as past studies from our lab have already demonstrated for the *Listeria* system (Buchholz et al., 2013; Graef et al., 2014; Cho et al., 2017; Kretschmer et al., 2020) (*Figure 10a*). At day eight p.i., single cell-derived responses were recovered at 29.3% and 19.3% from LCMV-Arm or LCMV- Cl13 infection, respectively. The coefficient of variation (CV) of the absolute sizes of single-cell progeny recovered from spleens served as a means to quantify variability (*Figure 10b*). These were higher for single cell progenies than

## Results

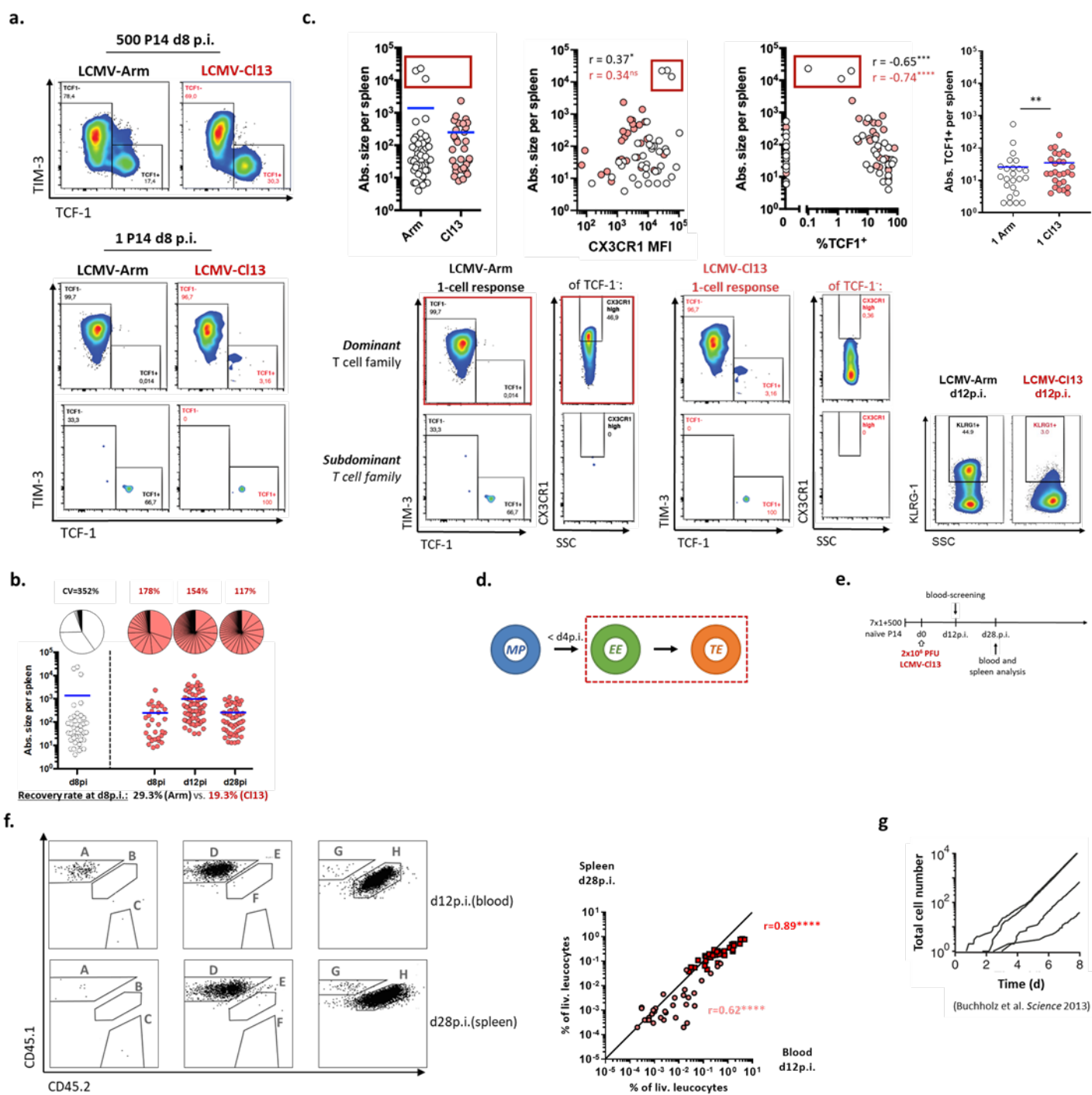


**Figure 10: Tracking of individual fates reveals impaired differentiation of terminal effectors and restricted variability in clonal burst size in chronic LCMV infection. a-g.**

**a.** Single cell-derived responses in chronic LCMV infection are variable.

**b.** Variability in clonal burst size is restricted in LCMV C113.

**c.** Single P14 fail to adopt an effector phenotype in chronic LCMV infection.

**d.** P14 differentiate progressively from MP to EE to TE during early LCMV infection.

**e.** Experimental scheme of longitudinal single cell fate mapping.

**f.** Stability in size is largely maintained among single cell responses throughout the first month of C113 infection.

**g.** Timing of fate decisions impacts proliferative output (Buchholz et al, 2013).

Data are representative for one of four (**a,c,f**) or compiled (**b,c,f**) of four independent experiments (**a-c**: n= 5 or six per group; **e**: n=11). Lines indicate mean. \* $r < 0.05$ , \*\*\* $r < 0.001$ , \*\*\*\* $r < 0.0001$  (Spearman non-parametric test).

for population controls (data not shown). Strikingly, the CV for single cells responding to LCMV-Arm infection was nearly two-fold that of their chronic counterpart. This appeared to be attributable to a few strongly expanded “giants”, which dominated the acute T-cell response and failed to develop in the context of chronic infection, thus limiting the CV (*Figure 10c*). These clones were negative for TCF-1 while strongly expressing CX3CR1, classifying them as TEs. In fact, once more mirroring observations from *Listeria*, there was a strongly negative correlation between MP phenotype indicated by TCF-1 and burst size (Buchholz et al., 2013) ( $r = -0,65^{***}$  in Arm and  $r = -0,74^{****}$  in Cl13) (*Figure 10c*). Additionally, the data showed a weakly positive correlation between burst size and MFI of CX3CR1 in Arm ( $r = 0,37^*$ ) (*Figure 10c*). No significant correlation manifested itself here in Cl13, due to the overall low expression of this marker in chronic infection, where the TCF-1<sup>+</sup> MPs and TCF-1<sup>-</sup>CX3CR1<sup>-</sup> EEs in turn constituted a greater proportion of the response. Thus, during early LCMV-infection, P14 differentiate progressively from MP to EE to TE (*Figure 10d*).

Experiments from later time points saw the greatest mean burst in Cl13 size at day twelve p.i., thus identifying a slightly delayed peak compared to day eight in acute infection (*Figure 10b*). A decline in burst size over time reflected gradual contraction of the initial response during the first month of infection. Relative progeny size between day twelve and 28p.i. were also correlated by longitudinal blood phenotyping (*Figure 10 f,g*). At day twelve, CX3CR1<sup>high</sup> cells were a prominent population during acute infection and stained positive for KLRG-1, while even at the peak of the exhausted immune response no TEs were discernible in Cl13 (*Figure 10c*).

In addition to confirm the absence of terminal effector differentiation during chronic infection on the single-cell level, these data underscored our assumption of an early onset of exhaustion. Mathematical modelling has previously indicated that such strongly expanded clones can only be generated by entering a highly proliferative subset soon after activation in order to allow for sufficiently high clonal output in a relatively short time span leading to analysis (Buchholz et al., 2013; Kretschmer et al., 2020) (*Figure 10g*).

## **4.2. scRNA-seq and RNA velocity analyses in early acute and chronic LCMV infection**

Analyzing the transcriptome of single cells has proven a potent source of information for early indicators of future fate decisions. Determining the ratio of unspliced vs. spliced RNA as

RNA velocities is another new and powerful tool to unmask developmental pathways. In a collaborative effort, our institute's biomathematicians (formerly AG Flossdorf) generated scRNAseq data for day six and analyzed them in the context of published data from day four and a half and eight post infection (Chen et al., 2019; Yao et al., 2019). These analyses were performed by Albulena Toska.

Representation of the data in the form of low-dimensional Uniform Manifold Approximation and Projection (UMAPs) revealed that after four and a half days in either acute or chronic infection, TCF-1<sup>-</sup> effector subsets had separated from TCF-1<sup>+</sup> MPs. Furthermore, although all cells initially grouped at similar areas of the map they could be readily separated according to the infection setting they had been isolated from by day 8 p.i. Leiden clustering identified seven distinct clusters, two of which – five and six – were enriched in the LCMV-Arm infection setting, while cluster three was associated with CI13 infection (*Figure 11a*). Cluster six consisted of the cells most highly enriched in KLRG-1. On a UMAP exclusively depicting cells recovered from chronic infection, the corresponding area appeared empty, consistent with our inability to find a significant TE response in this setting by flow-cytometry. Cells

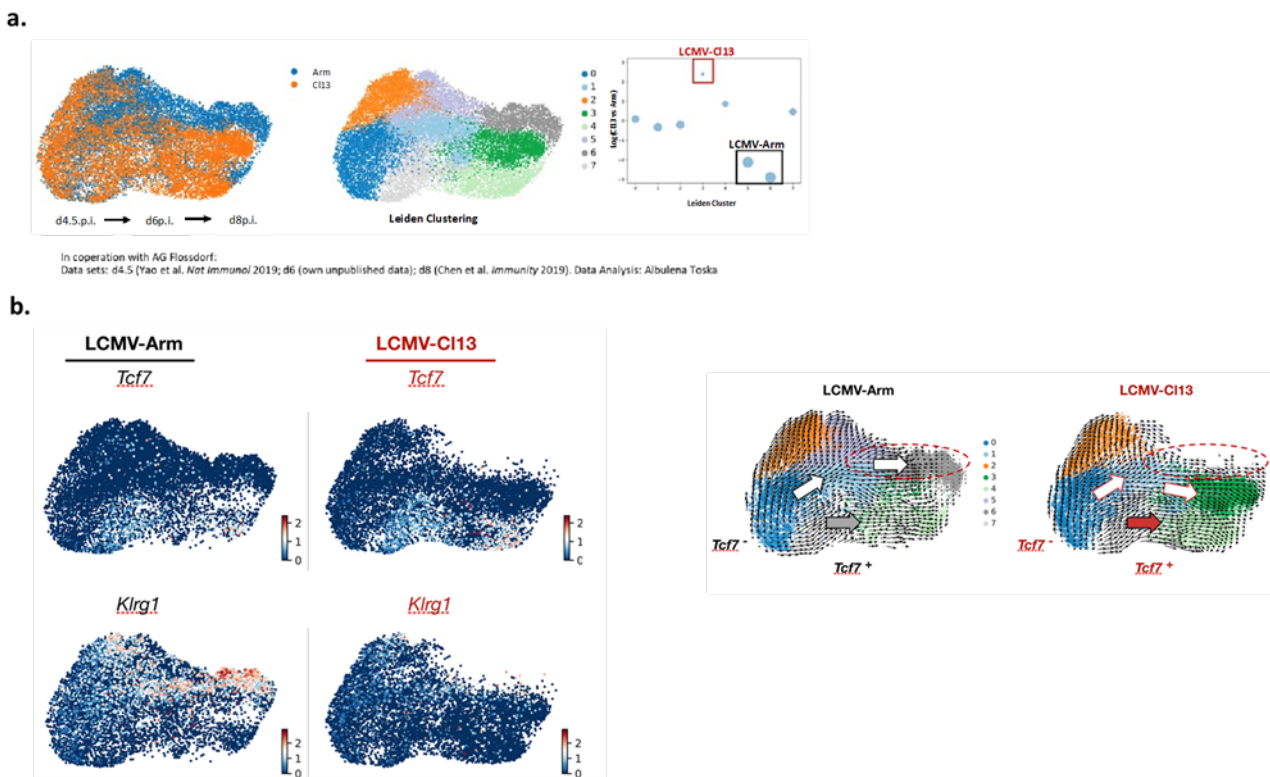


**Figure 11: sc-RNA-seq velocity analysis reveals distinct differentiation trajectories within the TCF7<sup>-</sup> T cell compartment in acute and chronic LCMV infection. a-b.**

**a.** P14 segregate into infection-specific clusters by day eight of Arm and CI13 infection.

**b.** TCF-7<sup>-</sup> effector cells embark on different trajectories in acute and chronic LCMV infection.

attributed to Cl13 clustered close to an area high in TCF-1, and for this population, too, there appeared a matching blank space on the UMAP of their functional counterpart (LCMV-Arm, Cluster 3). RNA velocities disclosed these infection specific clusters to be fed by the TCF-1<sup>-</sup> subset via distinct paths (*Figure 11b*). Taken together, these data provide further indication that the decision to lose expression of TCF-1 and adopt EE fate falls very early during acute and chronic infection, even before the divergence of differentiation trajectories of exhausted as compared to functional CD8<sup>+</sup> T cells between day 4.5 and day 8p.i. Furthermore, they predict a developmental pathway in which MPs first give rise to EEs, which in turn generate TEs.

### **4.3. Adoptive retransfer experiments of distinctly primed P14 cells**

#### **4.3.1 Early adoptive retransfer experiments to explore the developmental capacity of CD8<sup>+</sup> T cells exposed to chronic infection**

In order to experimentally verify the model proposed by our sc-RNA-seq velocities and explore the developmental capabilities of distinct T<sub>ex</sub> subsets early during LCMV infection, we performed a series of adoptive retransfers.

According to GFP-fluorescence reporting *Tcf7* transcription, we sorted MPs and EEs from day four and a half of either Armstrong or Clone 13 infection and intravenously transferred them into infection-matched recipients of the opposite infection strain (*Figure 12a*). Since no TEs exist at that point in chronic infection, we omitted this subset. The mice were sacrificed on day eight post infection and their spleens “speed-enriched” prior to further processing by staining solely for the congenic marker, CD45.1, and then triggering sorting on the respective channel, APC in this case (*Figure 12b*). This enabled us to subsequently assess the entire previously transferred population present among the splenocytes with high phenotypic resolution and within a reasonable timeframe. Generally, re-expansion proved superior in acute infection and MPs were more readily recovered than EEs (data not shown), consistent with a more differentiated subset being less suited to survive adoptive retransfer (Shin et al., 2007; Graef et al., 2014; Buchholz et al., 2016). Chronically primed cells, especially EEs, mounted a robust effector response after transfer to Arm-infected secondary hosts, indicating retained plasticity (*Figure 12c*). MPs gave rise to all three subsets, while no TCF-7<sup>+</sup> cells were present in the spleens of mice that had received TCF-7<sup>-</sup> EEs, as supported by a model of progressive differentiation (*Figure 10d*) (Buchholz et al., 2013; Kaech & Cui, 2012).

No cells expressed PD-1 or TOX as a residue of their priming (*Figure 12d*). Contrastingly, both subsets upregulated these exhaustion markers after being exposed to a chronic environment (*Figure 12d*). In contrast to MPs, EEs displayed a remarkable capacity to generate TEs, with this subset constituting about 25% of the immune response at the timepoint of analysis, testifying to their retained effector potential even after more than three days in the context of chronic infection (*Figure 12c*).

These observations ascribe a remarkable developmental plasticity to CD8<sup>+</sup> T cells recovered early during CI13 infection. At the same time, they confirm progressive differentiation from MP to EE and then TE for acute and chronic LCMV infection, with this final step being blocked in the latter case.

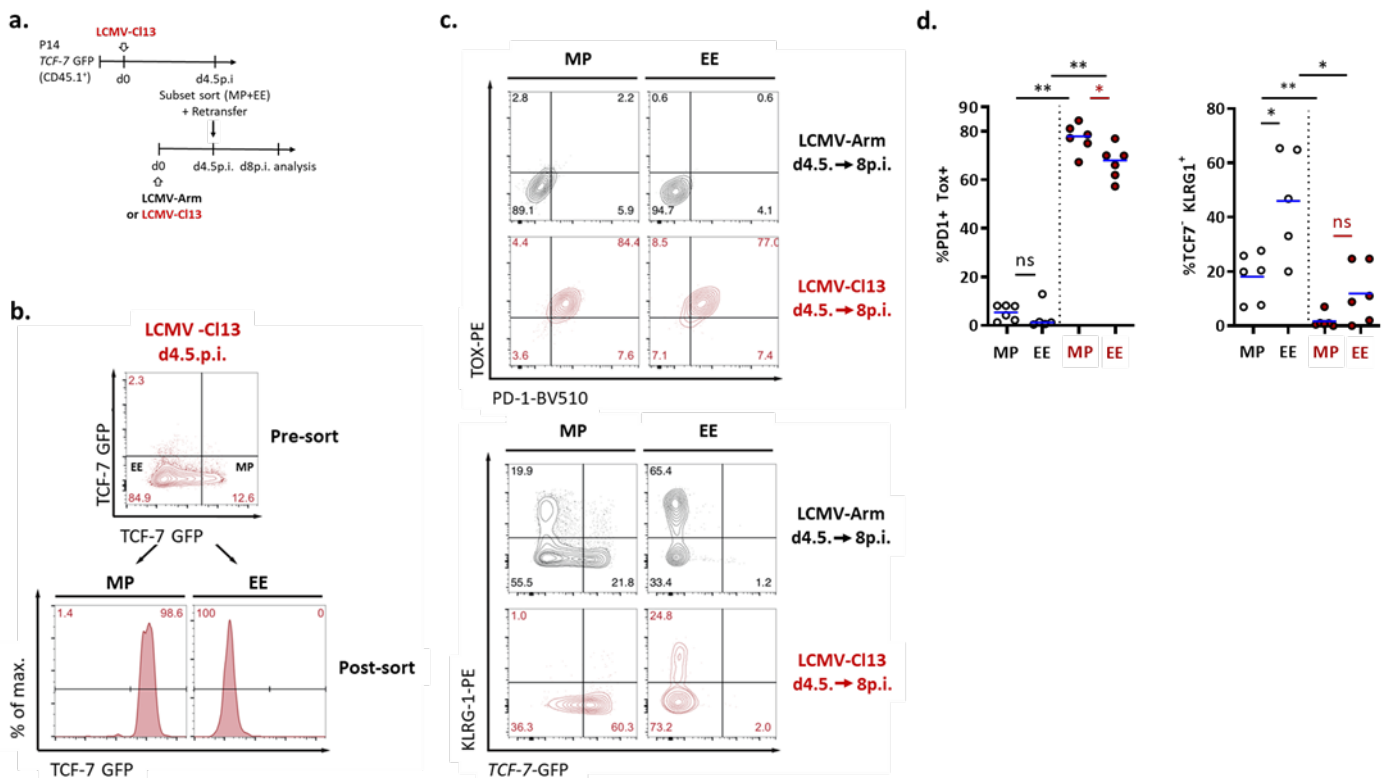


**Figure 12: MPs and EEs show considerable developmental plasticity at day four and half of CI13 infection. a-d.**

**a.** Experimental setup.

**b.** Sorting strategy.

**c-d.** Phenotype of chronically primed P14 at day eight p.i. after retransfer to either Arm or CI13 infection-matched recipients at day four and a half p.i.

Data are representative for one of two (**b-c**) or compiled of two (**d**) independent experiments (n=3 per group). Lines indicate mean. \*\*P < 0.01, \*P < 0.05 (Mann-Whitney test).

### 4.3.2 Transfer of acutely primed P14 subsets into chronic infection

The absence of terminally differentiated effector cells is a startling feature of chronic infection. Exhaustion is viewed as a distinct functional state tailored to limit immunopathology in settings of persistent antigenic stimulus (Virgin et al., 2009; Speiser et al., 2014). In light of this, we wondered about how TEs would behave if exposed to chronic infection and how their existence would impact the host and disease progression.

We primed P14-*TCF-7*-GFP reporter cells in primary recipients infected with Armstrong and sorted for MPs, EEs and TEs, identified by expression of *TCF-7* and *KLRG-1*, at the peak of the acute immune response on day eight p.i. (*Figure 13a*). Taking the low transfer efficacy for TEs into consideration, we then transferred all cells that could be sorted for each subset from the primary recipients intravenously into secondary hosts at day four and a half of either Cl13 or Arm infection (*Figure 13b*). Prior to sacrificing them at day eight post infection, they were monitored for weight loss and blood samples were collected to determine viral load. Lungs were fixed in PFA and evaluated for histopathological changes while speed-enriched splenocytes were either directly stained to evaluate phenotype or restimulated with cognate peptide to measure cytokine production. Transfer back into Arm confirmed a linear differentiation pattern and a high degree of functionality (*Figure 13c, d*). MPs and EEs subjected to the chronic setting upregulated TOX and PD-1 and did not give rise to TEs (*Figure 13c*). Contrastingly, TEs failed to adopt this chronic phenotype and largely retained their expression of *KLRG-1*. As expected, they did not replenish any other subset and the total number recovered was small. A slightly larger population could be found in the lung (data not shown), an organ effector cells are prone to home to on behalf of their chemokine-receptor profile (Galkina et al., 2005; Thatte et al., 2003). Expression of Granzyme A and B increased during progression along the differentiation trajectory, with TEs expressing the highest levels (*Figure 13e*). Functionally, both EEs and TEs produced larger amounts of IFN- $\gamma$ , while MPs contained the high percentage of cells positive for TNF- $\alpha$  (*Figure 13f*). There was no significant difference in weight loss. Average viral load was lowest after TE transfer, although the inter-subset differences did not reach statistical significance (*Figure 13g*). Possibly, the low quantity of surviving TEs compared to the other subsets tapered the magnitude of these differences.

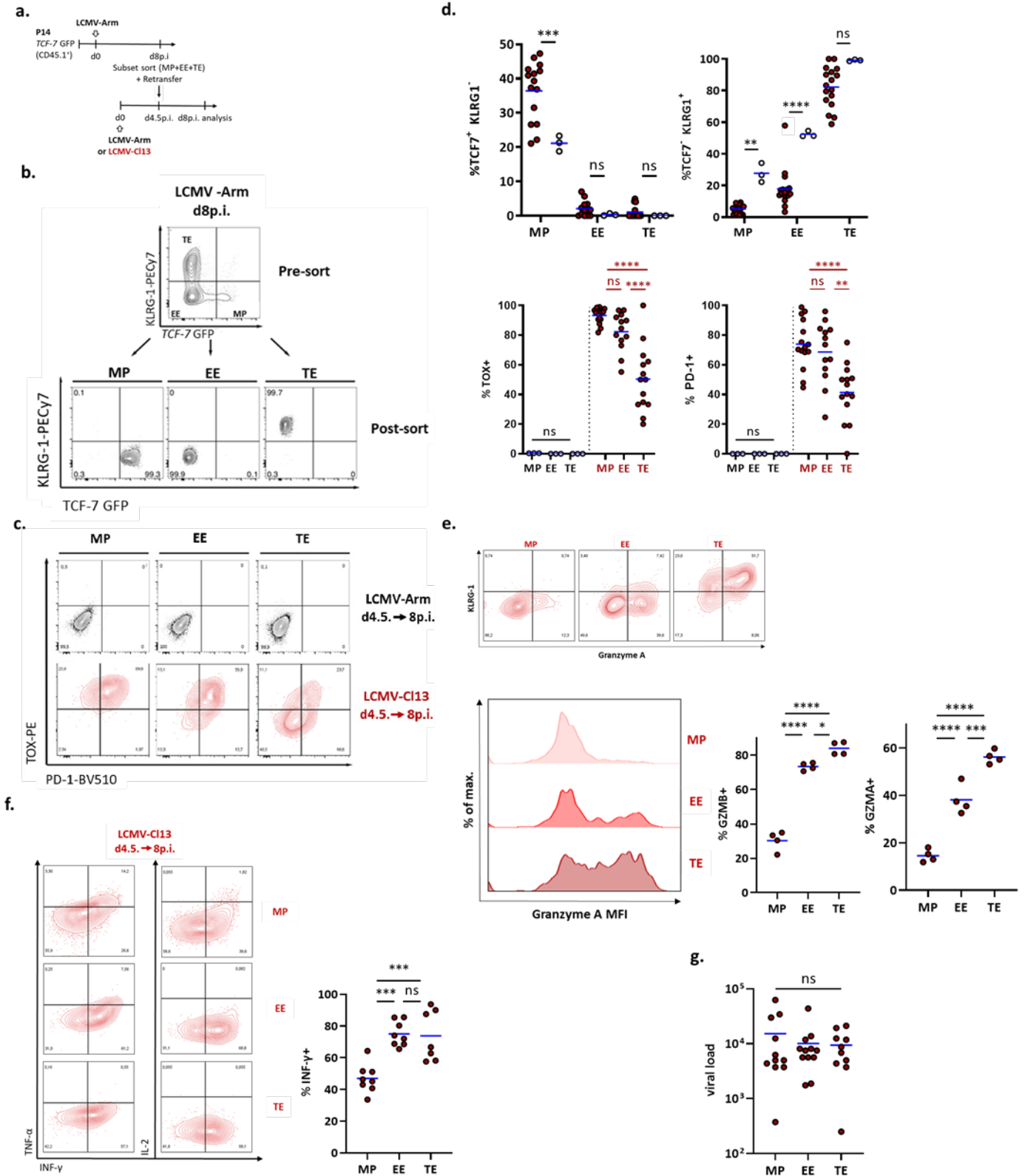


**Figure 13: Mature, acutely primed TEs appear exhaustion-resistant. a-g.**

**a.** Experimental setup.

**b.** Sorting strategy.

**c-d.** TEs exhibit the lowest levels of exhaustion markers and retain KLRG-1 expression.

**e.** Expression of both Granzyme A and B increases during differentiation from MP to EE to TE in CI13.

**f.** Acutely primed EEs and Tes maintain higher capability of cytokine production compared to MP in a chronic environment.

**g.** Viral load in chronically infected hosts after transfer of acutely primed distinct CD8<sup>+</sup> subsets.

Data are representative for or compiled of a single (**e**), two (**f**) or at least three (**b,c,d,g**) independent experiments (n=3-4 per group). Lines indicate mean. \*\*\*\*P < 0.0001, \*\*\*P < 0.001, \*\*P < 0.01, \*P < 0.05 (ANOVA).

Thus, mature TEs appear resistant to exhaustion and can be suspected to mediate superior virus control at the price of cytotoxic tissue damage.

#### 4.4. Longitudinal tracking of single cell progeny into the late phase of chronic infection

Despite focusing on the early dynamics of CD8<sup>+</sup> T cell exhaustion, single-cell *in vivo* fate mapping is equally applicable to the later stages of chronic infection. We transferred single cells, infected recipients with CI13 and subsequently screened their blood multiple times at day twelve, 28 and 120 days post infection before harvesting the spleens for ICCS at more

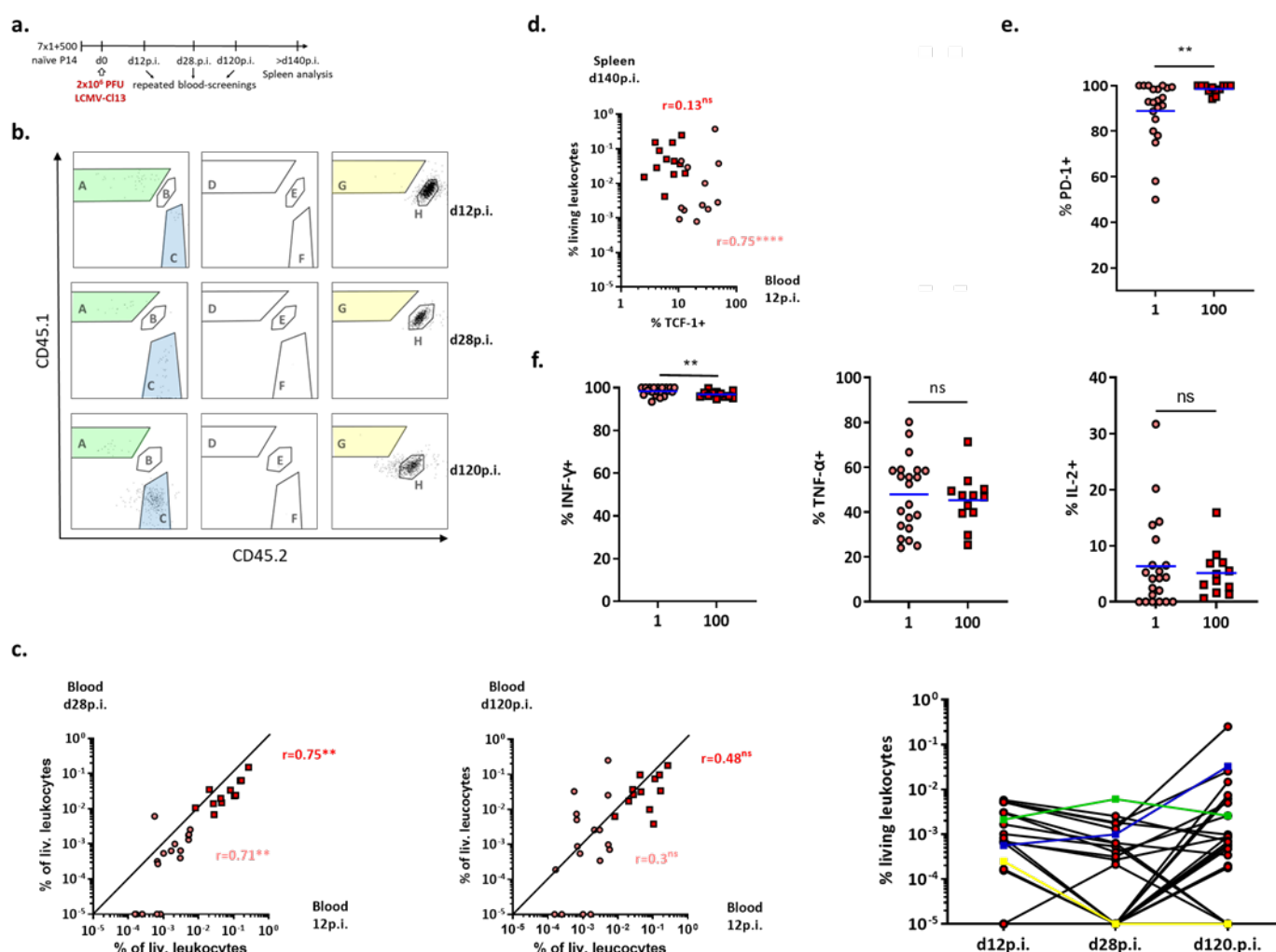


**Figure 14: Single cell fate mapping reveals that individual T cell families can revert to a functional state towards the late stages of LCMV CI13 infection. a-f.**

**a.** Experimental setup.

**b.** Example of three single cell progenies recovered at different timepoints in the same host.

**c.** Correlation of burst sizes throughout the course of infection and depiction of their development.

**d.** TCF-1 content early during CI13 infection indicates persistent into the late stage.

**e.** Individual clones downregulate PD-1 expression late in chronic infection (d140+p.i.).

**f.** P14 cells produce remarkable levels of effector cytokines in the late phase of CI13 infection. Data are representative for one of two (**b**) or compiled (**c-f**) of two independent experiments (n=7). Lines indicate means. \*\*\*\* $r < 0.0001$ , \*\* $r < 0.01$ , \* $r < 0.05$  (Spearman non-parametric test); \*\* $P < 0.05$ , \* $P < 0.01$  (Mann-Whitney test).

than 140 days post infection, when viremia could be expected to have been controlled in CD4<sup>+</sup> competent hosts (Wherry et al., 2003; Matloubian et al., 1990) (*Figure 14a*).

Indeed, viral titers in the blood were below the limit of detection at day 120p.i. (data not shown). The correlation of relative progeny size observed over the first month of infection did not persist until d120 p.i. (*Figure 14b, c*). Instead, TCF-1 content during the effector phase appeared to be a predictor of progeny size at the late stage (*Figure 14d*). As opposed to the 500 cell controls, which retained high levels of PD-1, individual single-cell progenies downregulated this marker to up to 50% (*Figure 14e*). The recovered progeny displayed a very functional phenotype, with nearly all cells being capable of IFN- $\gamma$  production and about half coproducing TNF- $\alpha$ . Absolute size and production of IL-2 were anticorrelated at d140 p.i., as would also be expected during the acute phase (*Figure 14f*). Taken together, CD8<sup>+</sup> T cells reacquire their effector capabilities after antigen clearance, a phenomenon that has been termed “resurgence” in a previous report (Fuller et al., 2004). Their ability to persist into the late stages of infection seems to be most accurately indicated by their initial content of the memory marker TCF-1.

## 5. Discussion

### 5.1. Progressive differentiation of exhausted CD8<sup>+</sup> T cells

Initially, exhausted CD8<sup>+</sup> T cells were assumed to originate from effector cells in case of ineffectual antigen clearance (Wherry et al., 2004), instead of either contracting or forming memory as after resolved infections (Kaech et al., 2002). As this idea does not satisfactorily explain either the timeliness of the initial phenotypic and functional changes or the heterogeneity within the T<sub>ex</sub> population, recently more refined concepts have been put forward. Collectively, those suggest a synergism between progenitor and progeny subsets to sustain the immune response to chronic infection (Utzschneider, Charmoy, et al., 2016; Paley et al., 2012; Beltra et al., 2020). We addressed the hitherto incompletely resolved questions of timing and early populations dynamics using single-cell *in vivo* fate mapping, sc-RNA-seq velocity analysis and adoptive retransfer experiments.

Investigating the abundance of the subsets revealed that MPs and EEs were readily detectable during the early phase of acute and chronic LCMV infection. In contrast, the generation of TE cells was relatively specific to T cell development during acute LCMV infection (*Figure 8b*). Exhaustion-specific changes manifested promptly. IL-2 production, which is a functional hallmark of bona fide memory T cells (Sallusto et al., 1999), was already reduced on day six p.i. (*Figure 8e*). Indeed, whereas MPs secreted the highest amount of this cytokine during acute LCMV infection, its production was markedly reduced during chronic LCMV infection. By day eight p.i., P14 T cells had acquired TOX and expressed PD-1 at higher MFI than their counterparts in the acute setting (*Figure 8b, f*). A clearly discernible MP population positive for TCF-1 was found in both infection settings, however, expression of CXCR5 within the MP compartment was specific to chronic infection, in line with previous findings (Im et al., 2016) (*Figure 7b*). The absolute as well as relative abundance of TCF1<sup>+</sup> precursors among offspring of single P14 that we detected were higher during CI13 compared to Arm infection (*Figure 10c*) support preferred generation in this setting due to higher levels of antigen (Utzschneider et al., 2020). As relative numbers were higher in CI13 on the population level as well, while no significant difference was observed for absolute numbers was detected (data not shown), increased retention of these cells in a progenitor state remains an alternative explanation (Verbeek et al., 1995; Utzschneider, Charmoy, et al.,

2016). Single cell data from day eight p.i. confirmed these phenotypical differences by showing a higher content of TCF-1<sup>+</sup> progeny among the cells recovered from LCMV-Cl13 infection (*Figure 10 a,c*). sc-RNA-seq velocity analyses showed a segregation of TCF-7<sup>+</sup> MPs from TCF-7<sup>-</sup> EEs already at day four and a half post infection, with the full establishment of distinct infection-specific clusters for Cl13 and Arm occurring up to day 8 p.i. (*Figure 11a*). Furthermore, it predicts KLRG-1<sup>+</sup> TEs to derive from the TCF-7<sup>-</sup> branch, as our adoptive retransfer confirmed experimentally (*Figure 11b*). Only MPs were able to repopulate all subsets while maintaining themselves following retransfer at day four and a half p.i., irrespective of the type of infection they were originally isolated from (*Figure 12c*). The same observations could be made after transfer into a chronic environment, albeit that in this case, no TEs emerged from either MPs or EEs.

At the late stage of Cl13 infection, markers of continuous antigenic stimulation are maintained upon rechallenge with Arm (Utzschneider et al., 2013). For early stages of chronic infection, however, our experimental data demonstrated significant developmental plasticity, strengthening the assumption that although first indicators are detectable very soon following vaccination, exhaustion is not fixed by initial priming (Brooks, McGavern, et al., 2006). MPs and EEs generated in chronic infection not only gave rise to KLRG-1<sup>+</sup> TEs, but downregulated PD-1 and TOX as well upon transfer into an acute setting at day four and a half p.i. When transferring those subsets to the environment of an early chronic infection, both subsets expressed significant levels of these markers (*Figure 12c, d*).

## 5.2. Clonal burst size is restricted in LCMV-Cl13

Single-cell derived responses in *L.m.* infection exhibit a high degree of variability regarding proliferation and differentiation, with large burst sizes corresponding to a prevalent TE phenotype of the respective progeny (Buchholz et al., 2013). Our present study confirms these findings for acute LCMV-Arm infection, during which the CD8<sup>+</sup> T-cell population appears to be dominated by few strongly expanded, highly effector-differentiated clones (*Figure 10c*). These “giants” reached cell counts of about 15 times the number of the next biggest clones; in graphical visualization, this imposes as a definite gap separating the two groups. Precisely such cells failed to develop in Cl13, leading to a reduced variability in clonal expansion compared to Arm (*Figure 10b*). The general principles of stochasticity of single cell-derived responses as well as a correlation between phenotype and burst size remained

applicable in this context (*Figure 10c*). This striking observation has implications for the temporal dynamics of CTL development in both acute and chronic infection. In order to generate "giants" up to day eight p.i., a particular clone will need to embark on a trajectory of vigorous division very soon after activation (*Figure 10g*). Proliferative activity increases downstream along the linear differentiation pathway, with TEs expanding at the greatest speed (Buchholz et al., 2013), an effect attributable to their increased and sustained sensitivity to IL-2, as opposed to memory precursors, which require a longer period of antigen availability for optimal expansion (Kretschmer et al., 2020). The fact that MPs are particularly sensitive to antigenic signals might explain why this subset is particularly prone to undergoing exhaustion programming, reflected in the previously described loss of IL-2 which is most pronounced in this subset. Thus, commitment to the TE lineage must be an early fate decision, which is selectively blocked in the initial stages of chronic infection. Utzschneider et al. (Utzschneider et al., 2020) detected TCF1<sup>+</sup>Tim-3<sup>+</sup> cells after the third division, and our RNA-seq and RNA-velocity analyses revealed that EEs had segregated from MPs by day four and a half p.i., hence before onset of the exhaustion program (*Figure 11a*). According to current opinion, exhaustion originates in the TCF-1<sup>+</sup> precursors, which then pass their exhaustion program on to their more differentiated TCF-1<sup>-</sup> descendants (Utzschneider et al., 2020). However, considering the burgeoning of EEs relative to the beginning of exhaustion temporally as well as the aforementioned subset-inherent differences in proliferative behavior, exclusively exhausting MPs should not prevent the formation of TEs. At this timepoint, they arose from preexisting EEs in our experiments. Consistent with this idea, progenitor and progeny would have to be targeted independently from one another to stop terminally differentiated, cytolytic cells from developing, demonstrating that exhaustion can be initiated in either subset independently. The modest TE populations transiently identifiable in the first days of LCMV-Cl13 infection display exhaustion-specific traits, such as CD39 expression, or could be offspring of such functional EEs that die off as the infection progresses (Utzschneider et al., 2020; Alfei et al., 2019).

### **5.3. Terminal effector differentiation is impaired in chronic infection**

Absence of effector cells is a distinctive feature of chronic infection (Joshi et al., 2007; Angelosanto et al., 2012). This defect in effector cell generation could be explained by either programming exhaustion/blocking effector differentiation with the TCF7<sup>+</sup> and/or the TCF7<sup>-</sup>

compartment. The trajectory, as identified by sc-RNA-seq-velocity analysis placed TEs as direct offspring of EEs (*Figure 11b*). Our single-cell data and early adoptive retransfer experiments confirmed this prediction, characterizing exhaustion as inhibiting this final differentiation step (*Figure 10d*).

Impediment of terminal differentiation has been attributed to TCF-1 (Chen et al., 2019) and TOX (Alfei et al., 2019; Khan et al., 2019), which modulate transcriptional circuitry to maintain precursor states. Recently, the relevance of BACH2 for the progenitor subset has been highlighted (Utzschneider et al., 2020; Yao et al., 2021), similar to its role in restricting senescence in acute infection (Roychoudhuri et al., 2016). In a similar vein, it has been implicated in prompting TE to revert to a KLRG-1<sup>-</sup> phenotype and transform into highly efficacious exKLRG-1 memory cells (Herndler-Brandstetter et al., 2018) subsequently to resolution of acute infection. PD-1 protects CD8<sup>+</sup> from overstimulation by an overwhelming quantity of antigen by mitigating TCR-activation (Odorizzi et al., 2015). Furthermore, PD-1 blockade acts by directing TCF-1<sup>+</sup> cells towards terminal differentiation, thereby transiently endowing them with enhanced cytotoxic functions (Pauken et al., 2016; Ghoneim et al., 2017). Mechanistically, this could be brought about by elevated nuclear levels of T-bet compared to Eomes after restored signal-transduction (McLane et al., 2019). In our hands, P14 cells failed to upregulate markers of senescence and cytotoxicity during chronic infection, compatible with dampened TCR-signaling due to high levels of PD-1 expression, of both on the population and the single cell level, in addition to displaying functional defects.

#### **5.4. KLRG-1<sup>+</sup> effector cells might hold immunopathogenic potential in the setting of chronic infection**

Exhaustion is a unique state of CD8<sup>+</sup> T cell differentiation, specifically adapted to poise viral control against cytotoxicity-mediated tissue damage during persistent antigenic stimulation (Speiser et al., 2014; Utzschneider et al., 2013). Immunopathology is associated with immunoreconstitutive treatment, such as PD-1 checkpoint inhibition, in mice (Frebel et al., 2012) and humans (Kumar et al., 2017), emphasizing the physiological necessity to curb effector functions under these conditions.

Previous work reported acutely primed, KLRG-1<sup>+</sup> cells unable to survive transfer into chronic infection for more than a week (Angelosanto et al., 2012), a finding that could be explained

irrespective of the type of infection by both their short-lived nature (Kaech et al., 2002) and limited capacity to survive adoptive retransfer (Graef et al., 2014). Due to these properties, it has so far not been possible to analyze phenotypic changes of KLRG1<sup>+</sup> TE cells, following transfer to a chronic infection environment. In this work, we addressed this open question by analyzing the complete splenic compartment of chronically infected recipient mice following transfer of MPs, EEs, and TEs. Notably, unlike MPs and EEs generated in Arm, acutely primed TEs failed to adopt an exhausted phenotype after exposure to Cl13, instead remaining positive for KLRG-1 and producing higher levels of effector cytokines compared to MPs (*Figure 13c, d*). But our data indicate that while this phenotypic and functional resistance to exhaustion might enable them to mediate superior viral control compared to MPs and EEs (*Figure 13g*), these enhanced cytolytic functions could come at the cost of immunopathology. Positive and negative consequences would likely be more pronounced if TEs were to continuously develop primarily in a setting of persistent antigen over an extended period, as might conceivably occur during checkpoint inhibitor treatment. Conceptually, our findings collectively bolster the understanding of exhaustion operating as a roadblock on terminal effector differentiation. This partly reflects the idea of the “arrested effector model” of T cell exhaustion, according to which the differentiation state of a cell at the onset of exhaustion determines its later functionality (Henning et al., 2018). Those already far enough along the differentiation trajectory at the time of its onset are no longer susceptible and keep speeding ahead unchecked, at the risk of potentially detrimental collateral damage. If they could be identified as likely culprits, this would not only help us to understand the etiology of immunopathology but also indicate potential approaches to prevent immune related Adverse Events (irAEs) as well as new avenues for adoptive cell therapies in the treatment of chronic infections and malignancies.

### **5.5. CD8<sup>+</sup> T cells regain functionality after clearance of LCMV-Cl13 from the blood**

Although CD4<sup>+</sup> depletion during infection with LCMV-Cl13 results in lifelong viremia, immunocompetent mice only show detectable titers in the blood for two to three months, after which virus only persists in certain organs such as the brain or the kidneys (Wherry et al., 2003; Ahmed et al., 1984), its course having been described as protracted rather than chronic under these circumstances (Fuller et al., 2004). Tracking of single cell-derived progeny far into the chronic phase of Cl13 infection led to several observations.

Firstly, while burst sizes correlated at day twelve and 28 p.i., indicating a stability in numbers during this phase, this could not be extrapolated up to the fifth month following vaccination, when blood borne virus was confirmedly non-detectable (*Figure 14b*). We observed a variety of different fates in distinct single cell-derived T cell families - that is, clonal burst sizes increasing, decreasing and remaining equal in size. These results suggest that contraction of antigen-specific CD8<sup>+</sup> T cells towards the later stages of chronic infection differentially affects individual T cell families. Instead, our work identifies a high percentage of TCF-1<sup>+</sup> MPs in the first month of infection as an indicator of long-term persistence, in line with this transcription factor maintaining the precursor subset and having stem-like qualities (Utzschneider, Charmoy, et al., 2016) (*Figure 14d*).

Secondly, we were surprised at the high level of functionality that cells exhibited during the very late stages of infection, according to both their phenotype and cytokine production, which both differed substantially from our prior observations at earlier timepoints. The high levels of IFN- $\gamma$ , TNF- $\alpha$  and even IL-2 were reminiscent of *bona fide* memory cells (*Figure 14f*). Unlike the responses mounted by the 100 cell control populations, some single cell progeny downregulate PD-1 expression to a level of 50% (*Figure 14e*). It is assumed that T<sub>ex</sub> cannot form true memory as they depend on the continued presence of antigen (Wherry et al., 2004). Similar to our own findings, another study reported reacquisition of effector functions after viral clearance (>139d p.i.) (Fuller et al., 2004). These discrepancies can at least partially be assigned to the different lengths of the resting periods (28 vs. approximately 50-80 days, assuming viral clearance between day 60 and 90). As “resurgence” of the immune response was affected by epitope-specificity and anatomic location, former abundance of antigen - presentation seemed to have an essential impact (Fuller et al., 2004). As administration of Highly Active Anti-Retroviral Therapy (HAART) during primary HIV infection has been shown to correspond with superior viral control relative to a delayed initiation of treatment (Oxenius et al., 2000; Rosenberg et al., 2000), the fact that CD8<sup>+</sup> T cells are not only able to regain functionality but that individual clones also lose their exhausted phenotype should be explored in future studies and could hold considerable therapeutical relevance.

Thus, the late phase of “protracted” Cl13 infection, several weeks after antigen clearance, not only saw P14 regain significant effector capabilities but also single clones to revert to a

functional phenotype, emphasizing the relevance of early treatment in preserving antiviral T cell response.

## 6. Summary

In situations of persistent antigenic stimulus, such as chronic viral infection and cancer, CD8<sup>+</sup> T cells adopt a hypofunctional state which has been termed “exhaustion”. It is characterized by stable expression of coinhibitory receptors, diminished cytokine production, metabolic impairment and as well as a unique transcriptional and epigenetic landscape.

Mechanistically, it prevents the formation of terminally differentiated effector cells, thereby exerting the important physiological function of limiting cytotoxicity and potentially fatal immunopathology. As exhaustion has been established as a distinct line of T cell development, different models regarding the various subsets which constitute the heterogeneous T<sub>ex</sub> pool, and their lineage trajectories were proposed. As many questions concerning early T cell diversification during chronic infection are still unresolved, we aimed to provide new insights using sc-RNA-seq-velocity analysis, adoptive retransfer experiments and single cell *in vivo* fate mapping within the murine LCMV infection model.

Our experimental data indicated CD8<sup>+</sup> T cells to segregate into three main populations early after vaccination with either acute or chronic LCMV- MP, EE and TE. We noted that, as opposed to observations from LCMV-Arm, CD8<sup>+</sup> T cell responses in LCMV-CI13 were not dominated by few strongly expanded, effector-differentiated clones. Although stochasticity on the single cell level and a correlation between expansion and TCF-1 expression analogous to acute infection was preserved, variability in clonal burst size was restricted. Additionally, cells from chronic LCMV infection lacked signs of terminal effector differentiation, such as expression of CX3CR1 or KLRG-1. Sc-RNA-seq velocity analysis suggested a progressive trajectory from MP to EE and then TE; we could confirm this prediction in adoptive retransfer experiments. Our scRNA-seq analysis and adoptive retransfer experiments also reveal that TCF7<sup>+</sup> and TCF7<sup>-</sup> cells have segregated before the exhaustion program is imprinted. Considering this early developmental separation, the exclusive exhaustion of MP cells should not preclude the generation of TEs. For this, EEs would need to undergo exhaustion reprogramming separate from MPs as well, demonstrating that exhaustion can arise in both compartments mutually independent. Remarkably, mature TEs appear exhaustion resistant upon exposure to an environment of persistent antigenic stimulus. Specifically, we suggest TEs as a possible cause of immunopathology in the context of chronic infection due to a retained higher level of functionality compared to MPs and EEs.

Their regulation could hold important implications for preventing immune related adverse events during immunoreconstitutive treatments such as checkpoint inhibition therapies.

---

**7. Bibliography**

1. Murphy, K., & Weaver, C. (2017). *Janeway's Immunobiology* (9th Edition ed.). Garland Science.
2. Kaech, S. M., Wherry, E. J., & Ahmed, R. Effector and memory T-cell differentiation: implications for vaccine development. *Nat Rev Immunol* **2**(4) 251-262 (2002).
3. Schluns, K. S., Kieper, W. C., Jameson, S. C., & Lefrançois, L. Interleukin-7 mediates the homeostasis of naïve and memory CD8 T cells in vivo. *Nature Immunology* **1**(5) 426-432 (2000).
4. Zhang, X., Sun, S., Hwang, I., Tough, D. F., & Sprent, J. Potent and Selective Stimulation of Memory-Phenotype CD8+ T Cells In Vivo by IL-15. *Immunity* **8**(5) 591-599 (1998).
5. Blair, D. A., Turner, D. L., Bose, T. O., Pham, Q. M., Bouchard, K. R., Williams, K. J., McAleer, J. P., Cauley, L. S., Vella, A. T., & Lefrancois, L. Duration of antigen availability influences the expansion and memory differentiation of T cells. *J Immunol* **187**(5) 2310-2321 (2011).
6. Prlic, M., Hernandez-Hoyos, G., & Bevan, M. J. Duration of the initial TCR stimulus controls the magnitude but not functionality of the CD8+ T cell response. *J Exp Med* **203**(9) 2135-2143 (2006).
7. van Stipdonk, M., Lemmens, E. & Schoenberger, S. . Naïve CTLs require a single brief period of antigenic stimulation for clonal expansion and differentiation. . *Nat Immunol* **2**(5) 423-429 (2001).
8. Joshi, N. S., Cui, W., Chandele, A., Lee, H. K., Urso, D. R., Hagman, J., Gapin, L., & Kaech, S. M. Inflammation directs memory precursor and short-lived effector CD8(+) T cell fates via the graded expression of T-bet transcription factor. *Immunity* **27**(2) 281-295 (2007).
9. Takemoto, N., Intlekofer, A. M., Northrup, J. T., Wherry, E. J., & Reiner, S. L. Cutting Edge: IL-12 inversely regulates T-bet and eomesodermin expression during pathogen-induced CD8+ T cell differentiation. *J Immunol* **177**(11) 7515-7519 (2006).
10. Cui, W., Joshi, N. S., Jiang, A., & Kaech, S. M. Effects of Signal 3 during CD8 T cell priming: Bystander production of IL-12 enhances effector T cell expansion but promotes terminal differentiation. *Vaccine* **27**(15) 2177-2187 (2009).
11. Starbeck-Miller, G. R., Xue, H. H., & Harty, J. T. IL-12 and type I interferon prolong the division of activated CD8 T cells by maintaining high-affinity IL-2 signaling in vivo. *J Exp Med* **211**(1) 105-120 (2014).

12. Zajac, A. J., Blattman, J. N., Murali-Krishna, K., Sourdive, D. J. D., Suresh, M., Altman, J. D., & Ahmed, R. Viral Immune Evasion Due to Persistence of Activated T Cells Without Effector Function. *Journal of Experimental Medicine* **188**(12) 2205-2213 (1998).
13. Wherry, E. J., Blattman, J. N., Murali-Krishna, K., van der Most, R., & Ahmed, R. Viral persistence alters CD8 T-cell immunodominance and tissue distribution and results in distinct stages of functional impairment. *J Virol* **77**(8) 4911-4927 (2003).
14. Utzschneider, D. T., Alfei, F., Roelli, P., Barras, D., Chennupati, V., Darbre, S., Delorenzi, M., Pinschewer, D. D., & Zehn, D. High antigen levels induce an exhausted phenotype in a chronic infection without impairing T cell expansion and survival. *J Exp Med* **213**(9) 1819-1834 (2016).
15. Bertoletti, A., & Gehring, A. J. The immune response during hepatitis B virus infection. *J Gen Virol* **87**(Pt 6) 1439-1449 (2006).
16. Ye, B., Liu, X., Li, X., Kong, H., Tian, L., & Chen, Y. T-cell exhaustion in chronic hepatitis B infection: current knowledge and clinical significance. *Cell Death Dis* **6** e1694 (2015).
17. Gruener, N. H., Lechner, F., Jung, M. C., Diepolder, H., Gerlach, T., Lauer, G., Walker, B., Sullivan, J., Phillips, R., Pape, G. R., & Klenerman, P. Sustained dysfunction of antiviral CD8+ T lymphocytes after infection with hepatitis C virus. *J Virol* **75**(12) 5550-5558 (2001).
18. Pauken, K. E., & Wherry, E. J. Overcoming T cell exhaustion in infection and cancer. *Trends in Immunology* **36**(4) 265-276 (2015).
19. Zarour, H. M. Reversing T-cell Dysfunction and Exhaustion in Cancer. *Clin Cancer Res* **22**(8) 1856-1864 (2016).
20. Virgin, H. W., Wherry, E. J., & Ahmed, R. Redefining chronic viral infection. *Cell* **138**(1) 30-50 (2009).
21. Allen, T. M., O'Connor, D. H., Jing, P., Dzuris, J. L., Mothé, B. R., Vogel, T. U., Dunphy, E., Liebl, M. E., Emerson, C., Wilson, N., Kunstman, K. J., Wang, X., Allison, D. B., Hughes, A. L., Desrosiers, R. C., Altman, J. D., Wolinsky, S. M., Sette, A., & Watkins, D. I. Tat-specific cytotoxic T lymphocytes select for SIV escape variants during resolution of primary viraemia. *Nature* **407**(6802) 386-390 (2000).
22. Scheppler, J. A., Nicholson, J. K., Swan, D. C., Ahmed-Ansari, A., & McDougal, J. S. Down-modulation of MHC-I in a CD4+ T cell line, CEM-E5, after HIV-1 infection. *The Journal of Immunology* **143**(9) 2858 (1989).

23. Kerkau, T., Schmitt-Landgraf, R., Schimpl, A., & Wecker, E. Downregulation of HLA Class I Antigens in HIV-1-Infected Cells. *AIDS Research and Human Retroviruses* **5**(6) 613-620 (1989).
24. Levitskaya, J., Sharipo, A., Leonchiks, A., Ciechanover, A., & Masucci Maria, G. Inhibition of ubiquitin/proteasome-dependent protein degradation by the Gly-Ala repeat domain of the Epstein-Barr virus nuclear antigen 1. *Proceedings of the National Academy of Sciences* **94**(23) 12616-12621 (1997).
25. Irmeler, M., Thome, M., Hahne, M., Schneider, P., Hofmann, K., Steiner, V., Bodmer, J.-L., Schröter, M., Burns, K., Mattmann, C., Rimoldi, D., French, L. E., & Tschopp, J. Inhibition of death receptor signals by cellular FLIP. *Nature* **388**(6638) 190-195 (1997).
26. Mueller, S. N., Matloubian, M., Clemens Daniel, M., Sharpe Arlene, H., Freeman Gordon, J., Gangappa, S., Larsen Christian, P., & Ahmed, R. Viral targeting of fibroblastic reticular cells contributes to immunosuppression and persistence during chronic infection. *Proceedings of the National Academy of Sciences* **104**(39) 15430-15435 (2007).
27. Brooks, D. G., Trifilo, M. J., Edelmann, K. H., Teyton, L., McGavern, D. B., & Oldstone, M. B. Interleukin-10 determines viral clearance or persistence in vivo. *Nat Med* **12**(11) 1301-1309 (2006).
28. van der Most, R. G., Murali-Krishna, K., Whitton, J. L., Oseroff, C., Alexander, J., Southwood, S., Sidney, J., Chesnut, R. W., Sette, A., & Ahmed, R. Identification of Db- and Kb-Restricted Subdominant Cytotoxic T-Cell Responses in Lymphocytic Choriomeningitis Virus-Infected Mice. *Virology* **240**(1) 158-167 (1998).
29. Zuniga, E. I., & Harker, J. A. T-cell exhaustion due to persistent antigen: quantity not quality? *Eur J Immunol* **42**(9) 2285-2289 (2012).
30. Richter, K., Brocker, T., & Oxenius, A. Antigen amount dictates CD8+ T-cell exhaustion during chronic viral infection irrespective of the type of antigen presenting cell. *Eur J Immunol* **42**(9) 2290-2304 (2012).
31. Mueller, S. N., & Ahmed, R. High antigen levels are the cause of T cell exhaustion during chronic viral infection. *Proceedings of the National Academy of Sciences* **106**(21) 8623-8628 (2009).
32. Wu, T., Ji, Y., Moseman, E. A., Xu, H. C., Manglani, M., Kirby, M., Anderson, S. M., Handon, R., Kenyon, E., Elkahlon, A., Wu, W., Lang, P. A., Gattinoni, L., McGavern, D. B., & Schwartzberg, P. L. The TCF1-Bcl6 axis counteracts type I interferon to repress exhaustion and maintain T cell stemness. *Sci Immunol* **1**(6) (2016).

33. Shin, H., Blackburn, S. D., Blattman, J. N., & Wherry, E. J. Viral antigen and extensive division maintain virus-specific CD8 T cells during chronic infection. *J Exp Med* **204**(4) 941-949 (2007).
34. Blattman, J. N., Wherry, E. J., Ha, S. J., van der Most, R. G., & Ahmed, R. Impact of epitope escape on PD-1 expression and CD8 T-cell exhaustion during chronic infection. *J Virol* **83**(9) 4386-4394 (2009).
35. Utzschneider, D. T., Gabriel, S. S., Chisanga, D., Gloury, R., Gubser, P. M., Vasanthakumar, A., Shi, W., & Kallies, A. Early precursor T cells establish and propagate T cell exhaustion in chronic infection. *Nat Immunol* **21**(10) 1256-1266 (2020).
36. Aichele, P., Neumann-Haefelin, C., Ehl, S., Thimme, R., Cathomen, T., Boerries, M., & Hofmann, M. Immunopathology caused by impaired CD8(+) T-cell responses. *Eur J Immunol* (2022).
37. Iwai, Y., Ishida, M., Tanaka, Y., Okazaki, T., Honjo, T., & Minato, N. Involvement of PD-L1 on tumor cells in the escape from host immune system and tumor immunotherapy by PD-L1 blockade. *Proceedings of the National Academy of Sciences* **99**(19) 12293-12297 (2002).
38. McLane, L. M., Abdel-Hakeem, M. S., & Wherry, E. J. CD8 T Cell Exhaustion During Chronic Viral Infection and Cancer. *Annu Rev Immunol* **37** 457-495 (2019).
39. Schietinger, A., Philip, M., Krisnawan, V. E., Chiu, E. Y., Delrow, J. J., Basom, R. S., Lauer, P., Brockstedt, D. G., Knoblaugh, S. E., Hammerling, G. J., Schell, T. D., Garbi, N., & Greenberg, P. D. Tumor-Specific T Cell Dysfunction Is a Dynamic Antigen-Driven Differentiation Program Initiated Early during Tumorigenesis. *Immunity* **45**(2) 389-401 (2016).
40. Day, C. L., Kaufmann, D. E., Kiepiela, P., Brown, J. A., Moodley, E. S., Reddy, S., Mackey, E. W., Miller, J. D., Leslie, A. J., DePierres, C., Mncube, Z., Duraiswamy, J., Zhu, B., Eichbaum, Q., Altfeld, M., Wherry, E. J., Coovadia, H. M., Goulder, P. J., Klenerman, P., . . . Walker, B. D. PD-1 expression on HIV-specific T cells is associated with T-cell exhaustion and disease progression. *Nature* **443**(7109) 350-354 (2006).
41. Shankar, P., Russo, M., Harnisch, B., Patterson, M., Skolnik, P., & Lieberman, J. Impaired function of circulating HIV-specific CD8+ T cells in chronic human immunodeficiency virus infection. *Blood* **96**(9) 3094-3101 (2000).
42. Speiser, D. E., Utzschneider, D. T., Oberle, S. G., Münz, C., Romero, P., & Zehn, D. T cell differentiations in chronic infection and cancer: functional adaption or exhaustion? *Nat Rev Immunol* (2014).

43. Okazaki, T., Chikuma, S., Iwai, Y., Fagarasan, S., & Honjo, T. A rheostat for immune responses: the unique properties of PD-1 and their advantages for clinical application. *Nat Immunol* **14**(12) 1212-1218 (2013).
44. Liang, S. C., Latchman, Y. E., Buhlmann, J. E., Tomczak, M. F., Horwitz, B. H., Freeman, G. J., & Sharpe, A. H. Regulation of PD-1, PD-L1, and PD-L2 expression during normal and autoimmune responses. *Eur J Immunol* **33**(10) 2706-2716 (2003).
45. Barber, D. L., Wherry, E. J., Masopust, D., Zhu, B., Allison, J. P., Sharpe, A. H., Freeman, G. J., & Ahmed, R. Restoring function in exhausted CD8 T cells during chronic viral infection. *Nature* **439**(7077) 682-687 (2006).
46. West, E. E., Jin, H. T., Rasheed, A. U., Penalzoza-Macmaster, P., Ha, S. J., Tan, W. G., Youngblood, B., Freeman, G. J., Smith, K. A., & Ahmed, R. PD-L1 blockade synergizes with IL-2 therapy in reinvigorating exhausted T cells. *J Clin Invest* **123**(6) 2604-2615 (2013).
47. Blackburn, S. D., Shin, H., Haining, W. N., Zou, T., Workman, C. J., Polley, A., Betts, M. R., Freeman, G. J., Vignali, D. A., & Wherry, E. J. Coregulation of CD8+ T cell exhaustion by multiple inhibitory receptors during chronic viral infection. *Nat Immunol* **10**(1) 29-37 (2009).
48. Pauken, K. E., Sammons, M. A., Odorizzi, P. M., Manne, S., Godec, J., Khan, O., Drake Adam, M., Chen, Z., Sen Debattama, R., Kurachi, M., Barnitz, R. A., Bartman, C., Bengsch, B., Huang Alexander, C., Schenkel Jason, M., Vahedi, G., Haining, W. N., Berger Shelley, L., & Wherry, E. J. Epigenetic stability of exhausted T cells limits durability of reinvigoration by PD-1 blockade. *Science* **354**(6316) 1160-1165 (2016).
49. Ghoneim, H. E., Fan, Y., Moustaki, A., Abdelsamed, H. A., Dash, P., Dogra, P., Carter, R., Awad, W., Neale, G., Thomas, P. G., & Youngblood, B. De Novo Epigenetic Programs Inhibit PD-1 Blockade-Mediated T Cell Rejuvenation. *Cell* **170**(1) 142-157 e119 (2017).
50. Frebel, H., Nindl, V., Schuepbach, R. A., Braunschweiler, T., Richter, K., Vogel, J., Wagner, C. A., Loffing-Cueni, D., Kurrer, M., Ludewig, B., & Oxenius, A. Programmed death 1 protects from fatal circulatory failure during systemic virus infection of mice. *J Exp Med* **209**(13) 2485-2499 (2012).
51. Buchholz, V. R., Flossdorf, M., Hensel, I., Kretschmer, L., Weissbrich, B., Gräf, P., Verschoor, A., Schiemann, M., Höfer, T., & Busch, D. H. Disparate Individual Fates Compose Robust CD8+ T Cell Immunity. *Science* **304** 630-635 (2013).

52. Graef, P., Buchholz, V. R., Stemberger, C., Flossdorf, M., Henkel, L., Schiemann, M., Drexler, I., Hofer, T., Riddell, S. R., & Busch, D. H. Serial transfer of single-cell-derived immunocompetence reveals stemness of CD8(+) central memory T cells. *Immunity* **41**(1) 116-126 (2014).
53. Sallusto, F., Lenig, D., Förster, R., Lipp, M., & Lanzavecchia, A. Two subsets of memory T lymphocytes with distinct homing potentials and effector functions. *Nature* **401**(6754) 708-712 (1999).
54. Verbeek, S., Izon, D., Hofhuis, F., Robanus-Maandag, E., te Riele, H., Watering, M. v. d., Oosterwegel, M., Wilson, A., Robson MacDonald, H., & Clevers, H. An HMG-box-containing T-cell factor required for thymocyte differentiation. *Nature* **374**(6517) 70-74 (1995).
55. Willinger, T., Freeman, T., Herbert, M., Hasegawa, H., McMichael, A. J., & Callan, M. F. Human naive CD8 T cells down-regulate expression of the WNT pathway transcription factors lymphoid enhancer binding factor 1 and transcription factor 7 (T cell factor-1) following antigen encounter in vitro and in vivo. *J Immunol* **176**(3) 1439-1446 (2006).
56. Utzschneider, D. T., Charmoy, M., Chennupati, V., Pousse, L., Ferreira, D. P., Calderon-Copete, S., Danilo, M., Alfei, F., Hofmann, M., Wieland, D., Pradervand, S., Thimme, R., Zehn, D., & Held, W. T Cell Factor 1-Expressing Memory-like CD8(+) T Cells Sustain the Immune Response to Chronic Viral Infections. *Immunity* **45**(2) 415-427 (2016).
57. Zhou, X., Yu, S., Zhao, D. M., Harty, J. T., Badovinac, V. P., & Xue, H. H. Differentiation and persistence of memory CD8(+) T cells depend on T cell factor 1. *Immunity* **33**(2) 229-240 (2010).
58. Jeannet, G., Boudousquie, C., Gardiol, N., Kang, J., Huelsken, J., & Held, W. Essential role of the Wnt pathway effector Tcf-1 for the establishment of functional CD8 T cell memory. *Proc Natl Acad Sci U S A* **107**(21) 9777-9782 (2010).
59. Chen, Z., Ji, Z., Ngiow, S. F., Manne, S., Cai, Z., Huang, A. C., Johnson, J., Staupe, R. P., Bengsch, B., Xu, C., Yu, S., Kurachi, M., Herati, R. S., Vella, L. A., Baxter, A. E., Wu, J. E., Khan, O., Beltra, J. C., Giles, J. R., . . . Wherry, E. J. TCF-1-Centered Transcriptional Network Drives an Effector versus Exhausted CD8 T Cell-Fate Decision. *Immunity* (2019).
60. Paley, M., A., Kroy, D., C., Odorizzi, P., M., Johnnidis, J., B., Dolfi, D., V., Barnett, B., E., Bikoff, E., K., Robertson, E., J., Lauer, G., M., Reiner, S., L., & Wherry, E. J. Progenitor and Terminal Subsets of CD8+ T Cells Cooperate to Contain Chronic Viral Infection. *Science* **338**(6111) 1220-1225 (2012).

61. He, R., Hou, S., Liu, C., Zhang, A., Bai, Q., Han, M., Yang, Y., Wei, G., Shen, T., Yang, X., Xu, L., Chen, X., Hao, Y., Wang, P., Zhu, C., Ou, J., Liang, H., Ni, T., Zhang, X., . . . Ye, L. Follicular CXCR5-expressing CD8(+) T cells curtail chronic viral infection. *Nature* **537**(7620) 412-428 (2016).
62. Im, S. J., Hashimoto, M., Gerner, M. Y., Lee, J., Kissick, H. T., Burger, M. C., Shan, Q., Hale, J. S., Lee, J., Nasti, T. H., Sharpe, A. H., Freeman, G. J., Germain, R. N., Nakaya, H. I., Xue, H. H., & Ahmed, R. Defining CD8+ T cells that provide the proliferative burst after PD-1 therapy. *Nature* **537**(7620) 417-421 (2016).
63. Beltra, J. C., Manne, S., Abdel-Hakeem, M. S., Kurachi, M., Giles, J. R., Chen, Z., Casella, V., Ngiow, S. F., Khan, O., Huang, Y. J., Yan, P., Nzingha, K., Xu, W., Amaravadi, R. K., Xu, X., Karakousis, G. C., Mitchell, T. C., Schuchter, L. M., Huang, A. C., & Wherry, E. J. Developmental Relationships of Four Exhausted CD8(+) T Cell Subsets Reveals Underlying Transcriptional and Epigenetic Landscape Control Mechanisms. *Immunity* **52**(5) 825-841 e828 (2020).
64. Yao, C., Lou, G., Sun, H. W., Zhu, Z., Sun, Y., Chen, Z., Chauss, D., Moseman, E. A., Cheng, J., D'Antonio, M. A., Shi, W., Shi, J., Kometani, K., Kurosaki, T., Wherry, E. J., Afzali, B., Gattinoni, L., Zhu, Y., McGavern, D. B., . . . Wu, T. BACH2 enforces the transcriptional and epigenetic programs of stem-like CD8(+) T cells. *Nat Immunol* **22**(3) 370-380 (2021).
65. Doering, T. A., Crawford, A., Angelosanto, J. M., Paley, M. A., Ziegler, C. G., & Wherry, E. J. Network analysis reveals centrally connected genes and pathways involved in CD8+ T cell exhaustion versus memory. *Immunity* **37**(6) 1130-1144 (2012).
66. McLane, L. M., Ngiow, S. F., Chen, Z., Attanasio, J., Manne, S., Ruthel, G., Wu, J. E., Staupe, R. P., Xu, W., Amaravadi, R. K., Xu, X., Karakousis, G. C., Mitchell, T. C., Schuchter, L. M., Huang, A. C., Freedman, B. D., Betts, M. R., & Wherry, E. J. Role of nuclear localization in the regulation and function of T-bet and Eomes in exhausted CD8 T cells. *Cell Rep* **35**(6) 109120 (2021).
67. Tsui, C., Kretschmer, L., Rapelius, S., Gabriel, S. S., Chisanga, D., Knopper, K., Utzschneider, D. T., Nussing, S., Liao, Y., Mason, T., Torres, S. V., Wilcox, S. A., Kanev, K., Jarosch, S., Leube, J., Nutt, S. L., Zehn, D., Parish, I. A., Kastenmuller, W., . . . Kallies, A. MYB orchestrates T cell exhaustion and response to checkpoint inhibition. *Nature* **609**(7926) 354-360 (2022).
68. Rollin, P. E., Nichol, S. T., Zaki, S., & Ksiazek, T. G. Arenaviruses and Filoviruses. *Manual of Clinical Microbiology* 1669-1686 (2015).

69. Vilibic-Cavlek, T., Savic, V., Ferenc, T., Mrzljak, A., Barbic, L., Bogdanic, M., Stevanovic, V., Tabain, I., Ferencak, I., & Zidovec-Lepej, S. Lymphocytic Choriomeningitis-Emerging Trends of a Neglected Virus: A Narrative Review. *Trop Med Infect Dis* **6**(2) (2021).
70. Muckenfuss, R. S., Armstrong, C., & Webster, L. T. ETIOLOGY OF THE 1933 EPIDEMIC OF ENCEPHALITIS. *Journal of the American Medical Association* **103**(10) 731-733 (1934).
71. Zhou, X., Ramachandran, S., Mann, M., & Popkin, D. L. Role of lymphocytic choriomeningitis virus (LCMV) in understanding viral immunology: past, present and future. *Viruses* **4**(11) 2650-2669 (2012).
72. Traub, E. A Filterable Virus Recovered from White Mice. *Science* **81**(2099) 298-299 (1935).
73. Ciurea, A., Klenerman, P., Hunziker, L., Horvath, E., Odermatt, B., Ochsenbein Adrian, F., Hengartner, H., & Zinkernagel Rolf, M. Persistence of lymphocytic choriomeningitis virus at very low levels in immune mice. *Proceedings of the National Academy of Sciences* **96**(21) 11964-11969 (1999).
74. Cole, G. A., Nathanson, N., & Prendergast, R. A. Requirement for  $\Theta$ -Bearing Cells in Lymphocytic Choriomeningitis Virus-induced Central Nervous System Disease. *Nature* **238**(5363) 335-337 (1972).
75. Lledó, L., Gegúndez, M. I., Saz, J. V., Bahamontes, N., & Beltrán, M. Lymphocytic choriomeningitis virus infection in a province of Spain: Analysis of sera from the general population and wild rodents. *Journal of Medical Virology* **70**(2) 273-275 (2003).
76. Bonthius, D. J. Lymphocytic Choriomeningitis Virus: An Underrecognized Cause of Neurologic Disease in the Fetus, Child, and Adult. *Seminars in Pediatric Neurology* **19**(3) 89-95 (2012).
77. Aebischer, O., Meylan, P., Kunz, S., & Lazor-Blanchet, C. Lymphocytic choriomeningitis virus infection induced by percutaneous exposure. *Occup Med (Lond)* **66**(2) 171-173 (2016).
78. Fischer, S. A., Graham, M. B., Kuehnert, M. J., Kotton, C. N., Srinivasan, A., Marty, F. M., Comer, J. A., Guarner, J., Paddock, C. D., DeMeo, D. L., Shieh, W.-J., Erickson, B. R., Bandy, U., DeMaria, A., Davis, J. P., Delmonico, F. L., Pavlin, B., Likos, A., Vincent, M. J., . . . Zaki, S. R. Transmission of Lymphocytic Choriomeningitis Virus by Organ Transplantation. *New England Journal of Medicine* **354**(21) 2235-2249 (2006).
79. Jamieson, D. J., Kourtis, A. P., Bell, M., & Rasmussen, S. A. Lymphocytic choriomeningitis virus: an emerging obstetric pathogen? *Am J Obstet Gynecol* **194**(6) 1532-1536 (2006).

80. Jamieson, B. D., Butler, L. D., & Ahmed, R. Effective clearance of a persistent viral infection requires cooperation between virus-specific Lyt2+ T cells and nonspecific bone marrow-derived cells. *Journal of Virology* **61**(12) 3930-3937 (1987).
81. Anderson, J., Byrne, J. A., Schreiber, R., Patterson, S., & Oldstone, M. B. Biology of cloned cytotoxic T lymphocytes specific for lymphocytic choriomeningitis virus: clearance of virus and in vitro properties. *Journal of Virology* **53**(2) 552-560 (1985).
82. Mims, C. A., & Blanden, R. V. Antiviral Action of Immune Lymphocytes in Mice Infected with Lymphocytic Choriomeningitis Virus. *Infection and Immunity* **6**(5) 695-698 (1972).
83. Ahmed, R., Salmi, A., Butler, L. D., Chiller, J. M., & Oldstone, M. B. Selection of genetic variants of lymphocytic choriomeningitis virus in spleens of persistently infected mice. Role in suppression of cytotoxic T lymphocyte response and viral persistence. *Journal of Experimental Medicine* **160**(2) 521-540 (1984).
84. Matloubian, M., Somasundaram, T., Kolhekar, S. R., Selvakumar, R., & Ahmed, R. Genetic basis of viral persistence: single amino acid change in the viral glycoprotein affects ability of lymphocytic choriomeningitis virus to persist in adult mice. *Journal of Experimental Medicine* **172**(4) 1043-1048 (1990).
85. Matloubian, M., Kolhekar, S. R., Somasundaram, T., & Ahmed, R. Molecular determinants of macrophage tropism and viral persistence: importance of single amino acid changes in the polymerase and glycoprotein of lymphocytic choriomeningitis virus. *Journal of Virology* **67**(12) 7340-7349 (1993).
86. Matloubian, M., Concepcion, R. J., & Ahmed, R. CD4+ T cells are required to sustain CD8+ cytotoxic T-cell responses during chronic viral infection. *Journal of Virology* **68**(12) 8056-8063 (1994).
87. Bergthaler, A., Flatz, L., Hegazy, A. N., Johnson, S., Horvath, E., Lohning, M., & Pinschewer, D. D. Viral replicative capacity is the primary determinant of lymphocytic choriomeningitis virus persistence and immunosuppression. *Proc Natl Acad Sci U S A* **107**(50) 21641-21646 (2010).
88. Smelt, S. C., Borrow, P., Kunz, S., Cao, W., Tishon, A., Lewicki, H., Campbell, K. P., & Oldstone, M. B. Differences in affinity of binding of lymphocytic choriomeningitis virus strains to the cellular receptor alpha-dystroglycan correlate with viral tropism and disease kinetics. *J Virol* **75**(1) 448-457 (2001).

89. Gairin, J. E., Mazarguil, H., Hudrisier, D., & Oldstone, M. B. Optimal lymphocytic choriomeningitis virus sequences restricted by H-2Db major histocompatibility complex class I molecules and presented to cytotoxic T lymphocytes. *Journal of Virology* **69**(4) 2297-2305 (1995).
90. Traub, E. PERSISTENCE OF LYMPHOCYTIC CHORIOMENINGITIS VIRUS IN IMMUNE ANIMALS AND ITS RELATION TO IMMUNITY. *The Journal of Experimental Medicine* **63**(6) 847-861 (1936).
91. Wherry, E. J., Ha, S.-J., Kaech, S. M., Haining, W. N., Sarkar, S., Kalia, V., Subramaniam, S., Blattman, J. N., Barber, D. L., & Ahmed, R. Molecular Signature of CD8+ T Cell Exhaustion during Chronic Viral Infection. *Immunity* **27**(4) 670-684 (2007).
92. Oldstone, M. B. A., Tishon, A., Chiller, J. M., Weigle, W. O., & Dixon, F. J. Effect of Chronic Viral Infection on the Immune System. *The Journal of Immunology* **110**(5) 1268 (1973).
93. Zinkernagel, R. M., & Doherty, P. C. Restriction of in vitro T cell-mediated cytotoxicity in lymphocytic choriomeningitis within a syngeneic or semiallogeneic system. *Nature* **248**(5450) 701-702 (1974).
94. Lau, L. L., Jamieson, B. D., Somasundaram, T., & Ahmed, R. Cytotoxic T-cell memory without antigen. *Nature* **369**(6482) 648-652 (1994).
95. Kägi, D., Ledermann, B., Bürki, K., Seiler, P., Odermatt, B., Olsen, K. J., Podack, E. R., Zinkernagel, R. M., & Hengartner, H. Cytotoxicity mediated by T cells and natural killer cells is greatly impaired in perforin-deficient mice. *Nature* **369**(6475) 31-37 (1994).
96. Masson, D., & Tschopp, J. Isolation of a lytic, pore-forming protein (perforin) from cytolytic T-lymphocytes. *Journal of Biological Chemistry* **260**(16) 9069-9072 (1985).
97. Gilden, D. H., Cole, G. A., & Nathanson, N. IMMUNOPATHOGENESIS OF ACUTE CENTRAL NERVOUS SYSTEM DISEASE PRODUCED BY LYMPHOCYTIC CHORIOMENINGITIS VIRUS : II. ADOPTIVE IMMUNIZATION OF VIRUS CARRIERS. *Journal of Experimental Medicine* **135**(4) 874-889 (1972).
98. Volkert, M., Bro-Jorgensen, K., & Marker, O. Persistent LCM virus infection in the mouse. Immunity and tolerance. *Bulletin of the World Health Organization* **52**(4-6) 471-478 (1975).
99. Oldstone, M. B. A., Nerenberg, M., Southern, P., Price, J., & Lewicki, H. Virus infection triggers insulin-dependent diabetes mellitus in a transgenic model: Role of anti-self (virus) immune response. *Cell* **65**(2) 319-331 (1991).

100. Ohashi, P. S., Oehen, S., Buerki, K., Pircher, H., Ohashi, C. T., Odermatt, B., Malissen, B., Zinkernagel, R. M., & Hengartner, H. Ablation of “tolerance” and induction of diabetes by virus infection in viral antigen transgenic mice. *Cell* **65**(2) 305-317 (1991).
101. Pfizenmaier, K., Trostmann, H., Röllinghoff, M., & Wagner, H. Temporary presence of self-reactive cytotoxic T lymphocytes during murine lymphocytic choriomeningitis. *Nature* **258**(5532) 238-240 (1975).
102. Reiner, S. L., Sallusto, F., & Lanzavecchia, A. Division of Labor with a Workforce of One: Challenges in Specifying Effector and Memory T Cell Fate. *Science* **317**(5838) 622-625 (2007).
103. Stemmerger, C., Huster, K. M., Koffler, M., Anderl, F., Schiemann, M., Wagner, H., & Busch, D. H. A single naive CD8+ T cell precursor can develop into diverse effector and memory subsets. *Immunity* **27**(6) 985-997 (2007).
104. Gerlach, C., van Heijst, J. W., Swart, E., Sie, D., Armstrong, N., Kerkhoven, R. M., Zehn, D., Bevan, M. J., Schepers, K., & Schumacher, T. N. One naive T cell, multiple fates in CD8+ T cell differentiation. *J Exp Med* **207**(6) 1235-1246 (2010).
105. Buchholz, V. R., Schumacher, T. N., & Busch, D. H. T Cell Fate at the Single-Cell Level. *Annu Rev Immunol* **34** 65-92 (2016).
106. Chang John, T., Palanivel Vikram, R., Kinjyo, I., Schambach, F., Intlekofer Andrew, M., Banerjee, A., Longworth Sarah, A., Vinup Kristine, E., Mrass, P., Oliaro, J., Killeen, N., Orange Jordan, S., Russell Sarah, M., Weninger, W., & Reiner Steven, L. Asymmetric T Lymphocyte Division in the Initiation of Adaptive Immune Responses. *Science* **315**(5819) 1687-1691 (2007).
107. Ahmed, R., & Gray, D. Immunological Memory and Protective Immunity: Understanding Their Relation. *Science* **272**(5258) 54-60 (1996).
108. Opferman, J. T., Ober Bertram, T., & Ashton-Rickardt Philip, G. Linear Differentiation of Cytotoxic Effectors into Memory T Lymphocytes. *Science* **283**(5408) 1745-1748 (1999).
109. Lanzavecchia, A., & Sallusto, F. Dynamics of T Lymphocyte Responses: Intermediates, Effectors, and Memory Cells. *Science* **290**(5489) 92-97 (2000).
110. Gerlach, C., Rohr Jan, C., Perié, L., van Rooij, N., van Heijst Jeroen, W. J., Velds, A., Urbanus, J., Naik Shalin, H., Jacobs, H., Beltman Joost, B., de Boer Rob, J., & Schumacher Ton, N. M. Heterogeneous Differentiation Patterns of Individual CD8+ T Cells. *Science* **340**(6132) 635-639 (2013).

111. Weber, K., Thomaschewski, M., Warlich, M., Volz, T., Cornils, K., Niebuhr, B., Tager, M., Lutgehetmann, M., Pollok, J. M., Stocking, C., Dandri, M., Benten, D., & Fehse, B. RGB marking facilitates multicolor clonal cell tracking. *Nat Med* **17**(4) 504-509 (2011).
112. Alfei, F., Kanev, K., Hofmann, M., Wu, M., Ghoneim, H. E., Roelli, P., Utzschneider, D. T., von Hoesslin, M., Cullen, J. G., Fan, Y., Eisenberg, V., Wohlleber, D., Steiger, K., Merkler, D., Delorenzi, M., Knolle, P. A., Cohen, C. J., Thimme, R., Youngblood, B., & Zehn, D. TOX reinforces the phenotype and longevity of exhausted T cells in chronic viral infection. *Nature* **571**(7764) 265-269 (2019).
113. Shin, H., & Wherry, E. J. CD8 T cell dysfunction during chronic viral infection. *Curr Opin Immunol* **19**(4) 408-415 (2007).
114. Henning, A. N., Roychoudhuri, R., & Restifo, N. P. Epigenetic control of CD8(+) T cell differentiation. *Nat Rev Immunol* (2018).
115. Yao, C., Sun, H. W., Lacey, N. E., Ji, Y., Moseman, E. A., Shih, H. Y., Heuston, E. F., Kirby, M., Anderson, S., Cheng, J., Khan, O., Handon, R., Reilley, J., Fioravanti, J., Hu, J., Gossa, S., Wherry, E. J., Gattinoni, L., McGavern, D. B., . . . Wu, T. Single-cell RNA-seq reveals TOX as a key regulator of CD8(+) T cell persistence in chronic infection. *Nat Immunol* **20**(7) 890-901 (2019).
116. Böttcher, J. P., Beyer, M., Meissner, F., Abdullah, Z., Sander, J., Hochst, B., Eickhoff, S., Rieckmann, J. C., Russo, C., Bauer, T., Flecken, T., Giesen, D., Engel, D., Jung, S., Busch, D. H., Protzer, U., Thimme, R., Mann, M., Kurts, C., . . . Knolle, P. A. Functional classification of memory CD8(+) T cells by CX3CR1 expression. *Nat Commun* **6** 8306 (2015).
117. Gerlach, C., Moseman, E. A., Loughhead, S. M., Alvarez, D., Zwijnenburg, A. J., Waanders, L., Garg, R., de la Torre, J. C., & von Andrian, U. H. The Chemokine Receptor CX3CR1 Defines Three Antigen-Experienced CD8 T Cell Subsets with Distinct Roles in Immune Surveillance and Homeostasis. *Immunity* **45**(6) 1270-1284 (2016).
118. Oestreich, K. J., Yoon, H., Ahmed, R., & Boss, J. M. NFATc1 Regulates PD-1 Expression upon T Cell Activation. *The Journal of Immunology* **181**(7) 4832 (2008).
119. Yokosuka, T., Takamatsu, M., Kobayashi-Imanishi, W., Hashimoto-Tane, A., Azuma, M., & Saito, T. Programmed cell death 1 forms negative costimulatory microclusters that directly inhibit T cell receptor signaling by recruiting phosphatase SHP2. *J Exp Med* **209**(6) 1201-1217 (2012).
120. Khan, O., Giles, J. R., McDonald, S., Manne, S., Ngiow, S. F., Patel, K. P., Werner, M. T., Huang, A. C., Alexander, K. A., Wu, J. E., Attanasio, J., Yan, P., George, S. M., Bengsch, B., Staupé, R. P.,

- Donahue, G., Xu, W., Amaravadi, R. K., Xu, X., . . . Wherry, E. J. TOX transcriptionally and epigenetically programs CD8(+) T cell exhaustion. *Nature* **571**(7764) 211-218 (2019).
121. Lu, P., Youngblood, B. A., Austin, J. W., Mohammed, A. U., Butler, R., Ahmed, R., & Boss, J. M. Blimp-1 represses CD8 T cell expression of PD-1 using a feed-forward transcriptional circuit during acute viral infection. *J Exp Med* **211**(3) 515-527 (2014).
122. Jenkins, M. K., & Moon, J. J. The role of naive T cell precursor frequency and recruitment in dictating immune response magnitude. *J Immunol* **188**(9) 4135-4140 (2012).
123. Blattman, J. N., Antia, R., Sourdive, D. J. D., Wang, X., Kaech, S. M., Murali-Krishna, K., Altman, J. D., & Ahmed, R. Estimating the Precursor Frequency of Naive Antigen-specific CD8 T Cells. *The Journal of Experimental Medicine* **195**(5) 657-664 (2002).
124. DiSanto, J. P., Klein, J. S., & Flomenberg, N. Phosphorylation and down-regulation of CD4 and CD8 in human CTLs and mouse L cells. *Immunogenetics* **30**(6) 494-501 (1989).
125. Altin, J. G., & Sloan, E. K. The role of CD45 and CD45-associated molecules in T cell activation. *Immunology & Cell Biology* **75**(5) 430-445 (1997).
126. Haeryfar, S. M., & Hoskin, D. W. Thy-1: more than a mouse pan-T cell marker. *J Immunol* **173**(6) 3581-3588 (2004).
127. Valitutti, S., Müller, S., Cella, M., Padovan, E., & Lanzavecchia, A. Serial triggering of many T-cell receptors by a few peptide–MHC complexes. *Nature* **375**(6527) 148-151 (1995).
128. Valitutti, S., Müller, S., Dessing, M., & Lanzavecchia, A. Signal extinction and T cell repolarization in T helper cell-antigen-presenting cell conjugates. *European Journal of Immunology* **26**(9) 2012-2016 (1996).
129. Luton, F., Buferne, M., Davoust, J., Schmitt-Verhulst, A. M., & Boyer, C. Evidence for protein tyrosine kinase involvement in ligand-induced TCR/CD3 internalization and surface redistribution. *The Journal of Immunology* **153**(1) 63 (1994).
130. Cantrell, D. A., Davies, A. A., & Crumpton, M. J. Activators of protein kinase C down-regulate and phosphorylate the T3/T-cell antigen receptor complex of human T lymphocytes. *Proceedings of the National Academy of Sciences* **82**(23) 8158-8162 (1985).

131. Dietrich, J., Hou, X., Wegener, A. M., Pedersen, L. O., Odum, N., & Geisler, C. Molecular characterization of the di-leucine-based internalization motif of the T cell receptor. *J Biol Chem* **271**(19) 11441-11448 (1996).
132. Hommel, M., & Hodgkin, P. D. TCR affinity promotes CD8+ T cell expansion by regulating survival. *J Immunol* **179**(4) 2250-2260 (2007).
133. Boulter, J. M., Schmitz, N., Sewell, A. K., Godkin, A. J., Bachmann, M. F., & Gallimore, A. M. Potent T cell agonism mediated by a very rapid TCR/pMHC interaction. *Eur J Immunol* **37**(3) 798-806 (2007).
134. Cho, Y. L., Flossdorf, M., Kretschmer, L., Hofer, T., Busch, D. H., & Buchholz, V. R. TCR Signal Quality Modulates Fate Decisions of Single CD4+ T Cells in a Probabilistic Manner. *Cell Rep* **20**(4) 806-818 (2017).
135. Kretschmer, L., Flossdorf, M., Mir, J., Cho, Y. L., Plambeck, M., Treise, I., Toska, A., Heinzl, S., Schiemann, M., Busch, D. H., & Buchholz, V. R. Differential expansion of T central memory precursor and effector subsets is regulated by division speed. *Nat Commun* **11**(1) 113 (2020).
136. Kaech, S. M., & Cui, W. Transcriptional control of effector and memory CD8+ T cell differentiation. *Nat Rev Immunol* **12**(11) 749-761 (2012).
137. Galkina, E., Thatte, J., Dabak, V., Williams, M. B., Ley, K., & Braciale, T. J. Preferential migration of effector CD8+ T cells into the interstitium of the normal lung. *J Clin Invest* **115**(12) 3473-3483 (2005).
138. Thatte, J., Dabak, V., Williams, M. B., Braciale, T. J., & Ley, K. LFA-1 is required for retention of effector CD8 T cells in mouse lungs. *Blood* **101**(12) 4916-4922 (2003).
139. Fuller, M. J., Khanolkar, A., Tebo, A. E., & Zajac, A. J. Maintenance, loss, and resurgence of T cell responses during acute, protracted, and chronic viral infections. *J Immunol* **172**(7) 4204-4214 (2004).
140. Wherry, E. J., Barber Daniel, L., Kaech Susan, M., Blattman Joseph, N., & Ahmed, R. Antigen-independent memory CD8 T cells do not develop during chronic viral infection. *Proceedings of the National Academy of Sciences* **101**(45) 16004-16009 (2004).
141. Utzschneider, D. T., Legat, A., Fuertes Marraco, S. A., Carrie, L., Luescher, I., Speiser, D. E., & Zehn, D. T cells maintain an exhausted phenotype after antigen withdrawal and population reexpansion. *Nat Immunol* **14**(6) 603-610 (2013).

142. Brooks, D. G., McGavern, D. B., & Oldstone, M. B. Reprogramming of antiviral T cells prevents inactivation and restores T cell activity during persistent viral infection. *J Clin Invest* **116**(6) 1675-1685 (2006).
143. Angelosanto, J. M., Blackburn, S. D., Crawford, A., & Wherry, E. J. Progressive loss of memory T cell potential and commitment to exhaustion during chronic viral infection. *J Virol* **86**(15) 8161-8170 (2012).
144. Roychoudhuri, R., Clever, D., Li, P., Wakabayashi, Y., Quinn, K. M., Klebanoff, C. A., Ji, Y., Sukumar, M., Eil, R. L., Yu, Z., Spolski, R., Palmer, D. C., Pan, J. H., Patel, S. J., Macallan, D. C., Fabozzi, G., Shih, H. Y., Kanno, Y., Muto, A., . . . Restifo, N. P. BACH2 regulates CD8(+) T cell differentiation by controlling access of AP-1 factors to enhancers. *Nat Immunol* **17**(7) 851-860 (2016).
145. Herndler-Brandstetter, D., Ishigame, H., Shinnakasu, R., Plajer, V., Stecher, C., Zhao, J., Lietzenmayer, M., Kroehling, L., Takumi, A., Kometani, K., Inoue, T., Kluger, Y., Kaech, S. M., Kurosaki, T., Okada, T., & Flavell, R. A. KLRG1(+) Effector CD8(+) T Cells Lose KLRG1, Differentiate into All Memory T Cell Lineages, and Convey Enhanced Protective Immunity. *Immunity* **48**(4) 716-729 e718 (2018).
146. Odorizzi, P. M., Pauken, K. E., Paley, M. A., Sharpe, A., & Wherry, E. J. Genetic absence of PD-1 promotes accumulation of terminally differentiated exhausted CD8+ T cells. *J Exp Med* **212**(7) 1125-1137 (2015).
147. Kumar, V., Chaudhary, N., Garg, M., Floudas, C. S., Soni, P., & Chandra, A. B. Current Diagnosis and Management of Immune Related Adverse Events (irAEs) Induced by Immune Checkpoint Inhibitor Therapy. *Front Pharmacol* **8** 49 (2017).
148. Oxenius, A., Price, D. A., Easterbrook, P. J., O'Callaghan, C. A., Kelleher, A. D., Whelan, J. A., Sontag, G., Sewell, A. K., & Phillips, R. E. Early highly active antiretroviral therapy for acute HIV-1 infection preserves immune function of CD8+ and CD4+ T lymphocytes. *Proceedings of the National Academy of Sciences* **97**(7) 3382-3387 (2000).
149. Rosenberg, E. S., Altfeld, M., Poon, S. H., Phillips, M. N., Wilkes, B. M., Eldridge, R. L., Robbins, G. K., D'Aquila, R. T., Goulder, P. J. R., & Walker, B. D. Immune control of HIV-1 after early treatment of acute infection. *Nature* **407**(6803) 523-526 (2000).

## 8. Acknowledgements

*Many people deserve recognition for their manifold contributions to this thesis. Firstly, I sincerely thank Dr. Veit Buchholz and Prof. Dr. Dirk Busch for the opportunity to work on this project by giving me the chance to join their work group and institute, as well as supervising me during my research there. My time at the MIH has been a truly instructive, rewarding and formative experience which I am confident to benefit from in my future life, both personally and professionally. I owe another big “thank you” to Dr. Lorenz Kretschmer, who guided my everyday work in the lab and whose valuable input crucially shaped this project. All members of the AG Buchholz and a considerable number from the AG Busch are greatly appreciated for helping me in all sorts of different small and big ways. The same applies to our institute’s biomathematicians, especially their former leader Dr. Michael Floßdorf, who served as my mentor, and particularly Albulena Toska, for our rewarding cooperation. Further, I would like to acknowledge the important role of CyTUM and the AG Schiemann in conscientiously performing my cell sorting. Prof Dr. Dietmar Zehn’s group, at the School of Life Sciences in Weihenstephan for provided us not only with the initial batches of virus stock and mouse lines, but also critical expertise on LCMV without which this project could not have been realized.*

*Finally, I am profoundly grateful to my family and friends for their continuous and unfaltering moral support during these past years, foremost my parents Ingrid and Erich, as well as my brother Philipp.*